Title

Biocircuitry linked to exercise adaptations: impact of dose and inter-individual response heterogeneity

Authors

Jeremy S. McAdam,[1,2,3,10] Michael P. Craig,[4,10] Zachary A. Graham,[1,2,3,5] Brandon Peoples,[2] S. Craig Tuggle,[1,2] Regina S. Seay,[2] Kaleen M. Lavin[1,2,3], Amber B. Sullivan[2], Samia M. O'Bryan[2,3], Sufen Yang,[2] Devin J. Drummer,[2,3] Christian J. Kelley,[2] Kalyani Peri,[6] Margaret B. Bell,[2,3] Inmaculada Aban,[6] Gary R. Cutter,[1,2,6] Arash Mahyari,[1] Yuan Wen,[7,8,9] Jin Zhang,[4] Akshay Hira,[4] Timothy J. Broderick,[1,4,11] Madhavi Kadakia[4,11], Marcas M. Bamman[1,2,3,10,11,12,*]

Affiliations

[1]Healthspan, Resilience, and Performance Research, Florida Institute for Human and Machine Cognition, Pensacola, FL 32502, USA

[2]UAB Center for Exercise Medicine, University of Alabama at Birmingham, Birmingham, AL 35205, USA

[3]Department of Cell, Developmental, and Integrative Biology, University of Alabama at Birmingham, Birmingham, AL 35294, USA

[4]Boonshoft School of Medicine, Wright State University, Dayton, OH 45435, USA

[5]Birmingham VA Health Care System, Birmingham, AL 35233, USA

[6]Department of Biostatistics, University of Alabama at Birmingham, Birmingham, AL 35294, USA

[7]Center for Muscle Biology, University of Kentucky, Lexington, KY 40506, USA

[8]Department of Physiology, College of Medicine, University of Kentucky, Lexington, KY 40506, USA

[9]Division of Biomedical Informatics, Department of Internal Medicine, College of Medicine, University of Kentucky, Lexington, KY 40506, USA

[10]These authors (co-first) have contributed equally.

[11]Senior author

[12]Lead contact

[*]Corresponding author

Address for Correspondence

Marcas M. Bamman, PhD

Florida Institute for Human and Machine Cognition

40 S. Alcaniz St.

Pensacola, FL, USA 32502

mbamman@ihmc.org

In brief

We examined *in vivo* and *ex vivo* adaptations to two randomized exercise prescriptions. Individual response variability overshadowed dose dependent effects. Deep phenotyping and miR transcriptomics of serum exosomes and skeletal muscle enabled multidimensional modeling of integrated biocircuits linked to attaining clinically significant outcomes.

Summary

In a randomized, dose-response trial, we used molecular and phenomic profiling to compare responses to traditional (TRAD) endurance plus resistance training and high-intensity tactical training (HITT). Ninety-four participants (18-27 years) completed 12 weeks of TRAD or HITT followed by 4 weeks of detraining. While *in vivo* phenotype improvements were not dose-dependent, a few dose-dependent *ex vivo* muscle adaptations were overshadowed by wide-ranging inter-individual response heterogeneity (IRH). To address this, we established minimum clinically important difference (MCID) scores to classify participants by their attainment of MCIDs for functional muscle quality (fMQ) and cardiorespiratory fitness (CRF). Using differential gene expression (DGE) of muscle and exosomal microRNAs (miRs) and higher-order singular value decomposition (HOSVD), we mapped the molecular and phenomic biocircuitry of IRH. Nine miRs emerged as robust features of training adaptability, providing new insights into the integrated biocircuitry driving exercise adaptations and response heterogeneity.

Key words: exercise dosing, performance, miR, response heterogeneity, muscle, exosomes, modeling

INTRODUCTION

Current public health guidelines emphasize the importance of combining endurance and resistance training to promote fitness and exercise-induced health benefits. The 2018 U.S. Department of Health and Human Services (HHS) guidelines recommend at least 150 minutes per week of moderate intensity endurance exercise or 75 minutes per week of vigorous higher intensity endurance exercise, combined with 2 or more days per week of resistance exercise targeting all major muscle groups.[1] These endurance prescriptions typically focus on continuous, steady state endurance exercise.

As an alternative to continuous endurance training, high-intensity interval training (HIIT) has gained popularity for its time-efficient approach to achieving rapid fitness improvements. HIIT typically involves maximal or near maximal sprint intervals separated by brief, lower intensity recovery periods. A modified form of HIIT integrates circuits of explosive bodyweight movements and exercises with external resistance, executed with minimal rest. This approach engages more muscle groups, challenges balance and coordination, and aims to provide combined endurance and strength/power benefits. Such programs are widely used among athletes and in the military, including the US Marine Corps' High-Intensity Tactical Training (HITT).

For endurance exercise, single-mode comparative efficacy trials of moderate-intensity continuous training (MICT) vs. HIIT are numerous and range from healthy adults to chronic disease.[2–10] Studies of combined endurance and resistance training are limited and comparison to HITT is lacking. To fill this void, we conducted a randomized, comparative efficacy trial with three major aims. The first aim was to assess the effects of 12 weeks (3 d/wk) of traditional (TRAD) combined training versus HITT on *in vivo* physiological performance and body composition along with *ex vivo* muscle histology and mitochondrial function. These were linked to microRNA (miR) regulatory networks to map epigenetic adaptations. Training protocols were distinct stressors designed to elicit adaptations typical of both endurance and resistance training. Randomization was stratified by sex (assigned at birth) to account for sex as a biological variable. Our second aim sought to explore inter-individual response heterogeneity (IRH) by defining multidimensional biocircuits linked to IRH by integrating over 37,000 features consisting of

phenomic and time series miR profiles from serum-derived exosomes and skeletal muscle in both untrained and trained states. Our third aim was to define early phase (4 wk) detraining in muscle and parallel miR expression. In a participant subset, we previously published transcriptomic responses in serum extracellular vesicles (EVs) and skeletal muscle after a single bout of TRAD or HITT in the untrained state.[11] This is the first comprehensive efficacy trail comparing TRAD and HITT over multiple weeks of training and detraining.

RESULTS

Participant characteristics were similar across randomized prescriptions

As shown in **Figure 1A**, 94 participants completed the efficacy trial [TRAD: n=45 (22F/23M) and HITT: n=49 (28F/21M)] and 91 participants completed the detraining phase (TRAD: n=44; HITT: n=47). Baseline demographics and a targeted panel of serum anabolic/androgenic hormones and growth factors are summarized in **Figure 1B**. As expected, sex differences were observed in testosterone, DHEA, SHBG and androstenedione. Sex-stratified randomization resulted in no baseline differences between TRAD and HITT in any measurement except DHEA (p=0.023).

HITT and TRAD prescriptions were met

Session adherence was high in both groups (HITT: 94.3% ± 5.7%; TRAD: 93.7% ± 5.3%) and prescribed exercise intensities were achieved (see STAR METHODS), thus minimizing any potential impact of non-adherence on IRH or on dosing comparisons.

HITT and TRAD similarly improved *in vivo* physiological performance and body composition

Both TRAD and HITT yielded established indices of training-induced health and performance benefits, as indicated by main time effects ($p < 0.001$) for peak aerobic power (VO_2peak, 11%), mechanical power at VO_2peak (14%), peak anaerobic power (16%), upper and lower body strength (14-27%), and lower body power (29%) (**Table 1**). A group*time interaction (p=0.009) during the Wingate anaerobic power test indicated superior fatigue resistance in TRAD. Additionally, trends toward group*time interaction suggested greater gains in peak anaerobic power and upper body strength in HITT. Improvements in body composition were comparable between TRAD and HITT, with both reducing total body fat,

abdominal subcutaneous fat and visceral adipose tissue concomitant with gains in total body, thigh and arm lean mass (**Table 1**). Neither prescription induced detectable systemic inflammation (**Table 2**). Overall, TRAD and HITT were similarly efficacious in enhancing physiological performance and body composition.

HITT and TRAD elicited differential *ex vivo* adaptations in skeletal muscle

We observed significant group*time interactions indicating 2-fold greater myofiber hypertrophy in TRAD. Mean fiber cross-sectional area (fCSA) increased 20% in TRAD vs. 7% in HITT (p=0.008) while type II fCSA increased 20% in TRAD vs. 12% in HITT (p=0.018) (**Table 2**). A main time effect was observed for type I fCSA hypertrophy (12%) with no difference between groups (**Table 2**). Myofiber type distribution remained unchanged (**Table 2**). Muscle capillary angiogenesis increased overall, with a 14% rise in capillary contacts per type I myofiber and no differences between groups (**Table 2**). However, capillary contacts per type II myofiber increased 27% in TRAD vs. 10% in HITT. Capillary density remained unchanged in both groups, indicating capillary angiogenesis kept pace with hypertrophy. $Pax7^+$ muscle satellite cells (SCs) per 100 myofibers showed a significant group*time interaction, with a 93% increase pre- to post-training in TRAD vs. 27% in HITT (p=0.006) (**Table 2**). SC frequency per 100 type I myofibers rose 49% in TRAD with no change in HITT (p=0.025), while type II-associated SCs increased similarly in both groups (80% overall). For mitochondrial function, HITT increased intermyofibrillar (IMF) citrate synthase (CS) 44% vs. 13% in TRAD (group*time, p=0.024). Subsarcolemmal (SS) CS and total CS increased similarly in both groups. (**Table 2**). Normalizing complex I and IV activities to CS showed no changes, suggesting the primary effect was training-induced mitochondrial biogenesis rather than enhanced mitochondrial function. Taken together, this suggests the equal improvements in VO_2peak were linked to distinct peripheral muscle adaptations: TRAD increased perfusion capacity through greater capillary angiogenesis, while HITT enhanced IMF mitochondrial biogenesis.

Training state (untrained, trained) and exercise prescription (HITT, TRAD) influenced miR signatures of the acute exercise response

Muscle

Differential gene expression (DGE) analysis compared the miR profiles of TRAD (n=43) and HITT (n=47). Pre-exercise baseline muscle samples yielded only 3 differentially expressed (DE) miRs (miR-143-3p, miR-145-5p and miR-2776-3p), supporting sex-stratified randomization (**Table S1**). Across acute response time points (3h and 24h after exercise in muscle), the response was generally greater at 24h compared to 3h for both W0 and W12 (**Figure 2A**). At 24h post-exercise, the number of DE miRs appeared higher in TRAD at W0 (20 vs. 13) but higher in HITT at W12 (32 vs. 11), indicating distinct response patterns between the exercise doses. DE miRs were largely unique to TRAD or HITT with limited overlap (**Figure 2A**, "shared"). However, five DE miRs in the 24h acute response were shared across doses and training state (miR-7-5p, miR-142-3p, miR-223-3p, miR-3529-3p and miR-582-5p). These shared miRs appear to represent a general exercise response in muscle that persisted even after 12wk of training (**Table S1**). Notably, previous studies have identified miR-223-3p as responsive in both serum EVs and muscle and miR-582-5p as responsive to a single exercise bout in the untrained state. Among the shared miRs, miR-3529-3p is unique in having no reported link to exercise.[11]

Serum exosomes

In serum exosomes, analysis of pre-exercise baseline in TRAD vs. HITT yielded only 9 DE miR (**Table S1**). A marked early response in serum exosome miR levels was observed immediately post-exercise (0h) in both untrained and trained states (**Figure 2B**). Only one miR, miR-197-3p, was DE at all time points (0h, 3h, 24h) in both W0 and W12, and it was specific to the HITT group. miR-197-3p is a known exercise-responsive miR, known to be upregulated in plasma after a single bout of endurance or resistance exercise.[12,13] In TRAD, 127 and 107 unique miRs were DE at W0 and 12 (across 0, 3 or 24h), respectively with 59 DE miRs common to both time points. In HITT, 237 and 239 unique miRs were DE at W0 and W12, respectively (across 0, 3 or 24h) with 172 DE miRs common to both W0 and W12 (**Figure 2B**, **Table S1**). Among the DE miRs, 42 miRs were shared between TRAD and HITT. Of note, two of these shared miRs, miR-223-3p and miR-582-5p, were DE in both exosomes and muscle (**Figure 2A-**

2B, **Table S1**). Both miRs are known to be altered in response to exercise. Specifically, miR-223-3p was DE in serum-derived EVs 24h after a single exercise bout in the untrained state;[11] Previous studies have also reported its up-regulation in serum after marathon running and DE in serum after ~6 months of training.[14,15] miR-582-5p is downregulated in EVs after fatiguing freestyle swimming.[16–18]

Training state (untrained, trained) influenced overall acute exercise response miR signatures irrespective of exercise prescription

Since *in vivo* physiological performance and body composition adaptations were largely unaffected by exercise prescription (**Table 1**), we further examined the impact of training state on miR signatures in serum exosomes and muscle in the full cohort (n = 90). In muscle, a robust response was noted at 24h at both W0 (13 of 14 DE miRs) and W12 (20 of 24 DE miRs) (**Figure 2C, left**). Among the 38 total unique miRs DE in muscle, only miR-223-3p was shared between W0 (DE at 3h and 24h) and W12 (DE at 24h). Consistent with the prescription-specific analysis, the magnitude of response to exercise was greater in serum exosomes than in muscle. Extensive changes in exosomal miR levels were observed at 0h in both untrained (180 DE miRs) and trained (159 DE miRs) states (**Figure 2C, right**), collapsed across 0, 3 and 24h. Of these, 108 DE miRs were shared between untrained and trained states (**Figure 2C, right**), resulting in 231 unique exosomal miRs DE post-exercise. Forty-two of these 108 miRs were identical to the 42 shared between TRAD and HITT when analyzed separately (Figures 2B-C and Table S1). Of the 28 muscle miRs and 231 exosomal miRs altered with exercise, 12 miRs were shared across muscle and exosomes (**Figure 2C**). Of these, six are newly discovered exercise-responsive miRs (miR-181c-5p, miR-514a-3p, miR-3680-5p, miR-4684-3p, miR-4714-5p and miR-6082). The remaining six are well-characterized exercise responsive miRs showing DE in multiple tissue types (miR-142-5p, miR-146b-5p, miR-206, miR-223-3p, miR-424-5p and miR-582-5p) (**Table S1**).[16,18–24]

Exercise-responsive miRs target mRNAs in known exercise-related pathways

High confidence mRNA targets of DE miRs, identified via miRTarbase v9, were subjected to KEGG pathway enrichment analysis using Enrichr to identify predicted signaling pathways altered in response

to exercise. For the muscle acute response, we combined all muscle miRs DE in response to exercise (i.e. 3h and/or 24h post-exercise at W0 and/or W12; **Figure 2C, left**). As expected, high-confidence mRNA targets showed enrichment in typical exercise-related pathways including mTOR signaling (odds ratio = 7.32, combined score = 280.15, adjusted p = 2.57E-14) and AMPK signaling (odds ratio = 7.32, combined score = 154.24, adjusted p = 2.04E-09). Similarly, high-confidence mRNA targets of DE exosomal miR (**Figure 2C, right**) showed enrichment in mTOR (odds ratio = 10.25, combined score = 638.61, adjusted p = 5.53E-27) and AMPK (odds ratio = 9.18, combined score = 398.22, adjusted p = 5.80E-19) signaling.

We further analyzed muscle responses separately in untrained (**Figure S2A, Table S3**) and trained (**Figure S2B, Table S3**) states. High confidence mRNA targets in the untrained state mapped to multiple metabolic and pro-inflammatory pathways (**Figure S2A**), as well as pathways involved in cell cycle regulation (e.g., p53, PI3K-AKT, Hippo), capillary angiogenesis (HIF-1), and autophagy. Interestingly, the trained state acute response mapped to largely the same pathways (**Figure S2B, Table S3**). Among miRs with no prior known association to exercise responses, we identified miR-524-5p in the untrained state and 3 novel miRs in the trained state (miR-181c-5p, miR-183-5p and miR-421).

Sex differences are profound in miR signatures at baseline and following exercise

Sex differences were tested in serum exosome and muscle samples from W0 pre-exercise (fasted, morning, resting) in females and males. A total of 102 muscle and 42 exosomal miRs were DE between sexes (**Figure 2D**). This finding is consistent with previously reported sex differences in miR profiles in serum, as well as gonadal and nongonadal tissues.[25–28] Among these, six miRs (miR-15b-5p, miR-199a-3p, miR-199b-3p, miR-361-5p, miR-381-3p and miR-12116) differed by sex in both muscle and exosomes. Five have been previously linked to exercise and shown to differ between sexes[16,18–22,24,29]. However, miR-12116 has not been previously associated with exercise or sex differences.

Next, we explored sex differences in the acute miR responses to exercise. In muscle, the magnitude of the exercise response was similar between sexes (**Figure 2E, Table S1**) and was most pronounced at

24h in both untrained (W0) and trained (W12) states. While a few DE muscle miRs at 24h were shared by both sexes, the majority exhibited sex-dependent responses (**Figure 2E**). Four acute response DE miRs shared between sexes in both untrained and trained states (miR-142-3p, miR-223-3p, miR-3529-3p and miR-7-5p) (**Figure 2E, Table S1**) were also identified in the analysis of the combined sex cohort, suggesting a role for these miRs in the general muscle exercise response, independent of sex or training state.

In serum exosomes (**Figure 2F**), untrained females showed a robust acute exercise response immediately post-exercise (0h) with 114 DE miRs, while in untrained males the dominant response occurred at 24h post-exercise, with 153 DE miRs (**Figure 2F, Table S1**). In the trained state, there were no notable sex differences in the timing of acute exercise responses (**Figure 2F**). Fewer than half of the acute DE miR responses were shared across the sexes (**Figure 2F,** "shared"). Only miR-197-3p was DE at all time points (0h, 3h, 24h) at W0 and W12 and exclusively in males. Notably, only miR-223-3p exhibited differential regulation in both serum exosomes and muscle (**Figure 2E and 2F**, **Table S1**).

DETRAINING

Short-term detraining reversed some but not all ex vivo muscle tissue adaptations

Detraining induced myofiber atrophy was prevalent in HITT group as noted for type II and mean fCSA while no significant atrophy was observed in the TRAD group, **Table 2**). However, training-induced improvements in capillarization were retained in both TRAD and HITT, indicating relative short-term stability (**Table 2**). Conversely, training-induced increases in $Pax7^{+}$ SCs and indices of mitochondrial biogenesis were completely reversed after 4wk of detraining period (**Table 2)**.

A detraining miR signature is evident in muscle but not in serum exosomes

A significant detraining signature was evident in muscle with 34 DE miRs (**Figure 2G**)**,** 28 of which have known links to exercise (**Table S1**). Within-group follow up analysis revealed a more pronounced detraining signature in HITT (n=80) vs. TRAD (n=19), with minimal overlap (n=3) between the two prescriptions (**Figure 2G**). A robust network of high confidence mRNA targets was observed for miRs in

the detraining muscle signature (**Figure S2C**). Among these, three miRs (miR-148a-5p, miR-181C-5p and 450a-5p) had no prior linkage to exercise or detraining. Pathway Enrichment analysis (**Figure S2C**) for detraining muscle showed many of the same pathways found in the untrained (**Figure S2A**) and trained (**Figure S2B**) exercise responses, but with far greater transcript membership. Pathways unique to detraining included TNF, Ras, and Toll-like receptor signaling, indicating potential alterations in inflammation, cell survival, remodeling, and immune signaling in the early phase of muscle detraining. In contrast to muscle, detraining appeared to exert little impact on exosomal miR (**Fig. 2G, Table S1 and S3**).

INTER-INDIVIDUAL RESPONSE HETEROGENEITY

In vivo adaptations to training vary widely among individuals and are independent of exercise prescription

There has been a growing focus on understanding the significant variation in the individual response to exercise, with the goal of developing personalized exercise prescriptions to maximize health benefits and optimize individualized rehabilitation.[30,31] The combined training programs in this trial provided a unique opportunity to investigate inter-individual response heterogeneity (IRH) across clinically important indices of both endurance training adaptability [cardiorespiratory fitness (CRF), i.e., VO_2peak] and resistance training adaptability [functional muscle quality (fMQ), i.e., knee extensor strength normalized to DXA-derived thigh lean mass]. We applied a well-established distribution-based method[32] to define minimum clinically important difference (MCID) scores pre- to post-training in CRF and fMQ. Eighty-two participants were classified based on these MCID criteria shown in **Figures 3A-B**. Importantly, the proportions of participants attaining or exceeding these MCIDs were not biased by training prescription (HITT, TRAD) (**Figures 3A-B**), allowing us to pool all participants as one cohort to better interrogate IRH. Overall, 67% of participants attained the MCID for fMQ while 61% attained the CRF MCID. The distribution of participants achieving both MCIDs (39%), fMQ only (28%), CRF only (22%), or neither (11%) is summarized in the Punnett square (**Figure 3C**). From the initial cohort of 82 participants, we

downselected n=80 for DGE and n=75 for higher-order singular value decomposition (HOSVD) due to missing features needed for each analysis.

miRs differentially regulated in fMQ+/CRF+ target mRNAs in exercise related signaling pathways

The miR signatures of fMQ+/CRF+ dual responders (n=30) were compared to the remaining cohort (n=50). DGE analysis revealed a more pronounced acute (3h) exercise response in exosomes compared to muscle (**Figure 3D, Table S1**), with the fMQ+/CRF+ participants showing a relatively blunted trained response (W12). Among fMQ+/CRF+, 11 DE miRs were shared across the W0 and W12 exosome responses compared to 30 DE miRs among the other participants across these timepoints (**Figure 3D**). Cytoscape analysis revealed exosomal miR links to exercise which have not been previously reported. These include miR-181c-5p, miR-365a-3p, miR-496 and miR-935 in untrained acute response, and miR-34c-5p, miR-299-5p and miR-543 in the trained acute response (**Figure 3D, right**). No DE miRs were shared between muscle and exosomes. In contrast to the acute responses, the effect of training (*i.e.*, W12 baseline trained state vs. W0 baseline) was more evident in muscle, with more DE miRs in fMQ+/CRF+ vs. the others (31 and 8, respectively) (**Figure 3E**). The Cytoscape network of DE miRs from muscle in the fMQ+/CRF+ group included two not previously linked to exercise, miR-376b-3p and miR-483-3p. Similarly, the effect of detraining was more dominant in muscle, with no overlap in signatures between muscle and exosomes (**Figure 3F**). The fMQ+/CRF+ detraining network from muscle included three miRs not previously linked to exercise, miR-135b-3p, miR-194-3p and miR-361-5p. Pathway analysis of the high confidence mRNA targets of the DE miRs from signaling networks in **Figure 3** indicated enrichment in MAPK, PI3K-AKT, HIF-1, mTOR, and cell cycle regulatory pathways, among others (**Figure S3, Table S3**). Interestingly, longevity regulating pathway signaling was enriched in the acute and trained response for fMQ+/CRF+ participants but not in detraining.

HOSVD analysis reveals in vivo and ex vivo phenomic features associated with fMQ+/CRF+ responder status

We leveraged HOSVD to define multidimensional biocircuitry by integrating all phenomic, ex vivo, and

molecular features (**Figure 4**) linked to the dual responder fMQ+/CRF+ classification (**Figure 4A,** Punnett sub-square shaded blue) versus all others (**Figure 4A** Punnett sub-squares shaded white). CRF+/- and fMQ+/- responder status was not biased by sex. The HOSVD model incorporated over 37,000 features across the categories in **Figure 4B**. Top phenomic features are summarized in **Figure 4C** (directionality of each arrow indicates fMQ+/CRF+ vs. all others). Interestingly, the majority linked to MCID attainment were baseline pre-training features. At baseline, fMQ+/CRF+ group reported lower physical activity, with 58% identifying as sedentary compared to 29% in other groups. Additionally, 81% of the fMQ+/CRF+ participants reported low workplace physical demands, compared to vs. 59% in the remaining cohort. Habitual caffeine (coffee, tea, soda) consumption was lower as 58% of fMQ+/CRF+ reported none (vs. 35%). Habitual alcohol intake was also lower in fMQ+/CRF+ with 46% (vs. 33%) reporting no regular consumption. For performance, knee extensor fatigability was lower in fMQ+/CRF+ as they were able to sustain a higher proportion of peak work during repeated, maximal isotonic knee extension contractions. Android adiposity at baseline was lower in the fMQ+/CRF+ group and, although no overt inflammation was detected, circulating IL-6 levels were slightly lower in fMQ+/CRF+ (~0.122 pg/mL). Via muscle tissue analyses ex vivo, fMQ+/CRF+ had lower baseline muscle capillary density (246 vs. 268 cap/mm^2) and fewer capillary contacts per type I myofiber (3.84 vs. 4.08).

The dominant training-induced *in vivo* phenotype difference between fMQ+/CRF+ and all others was the magnitude of reduction in android adiposity, as fMQ+/CRF+ participants experienced greater loss of android fat by numerous measures. In muscle, capillarization increased to a greater extent in fMQ+/CRF+ which may reflect the lower starting point.

HOSVD analysis reveals a differential resting and acute response miR expression profiles associated with fMQ+/CRF+

Downselection of the top 5% of features in the top 10 LVs identified 524 miR features highly associated with fMQ+/CRF+ (**Figures 4D and 4E**), with 236 DE miRs noted in muscle alone, 258 in serum exosomes alone, and 30 shared between tissues. **Figure 4D** highlights the 222 DE miRs (132 in muscle,

90 in exosomes) detected under resting conditions (fasted, morning pre-exercise at W0 or W12). In resting muscle, 65 DE miRs were detected at W0 with 67 at W12 (overall, 50 higher and 82 lower in fMQ+/CRF+). Among the 90 exosomal DE miRs, 54 were detected at W0 and 36 at W12 (overall, 43 were higher and 47 lower in fMQ+/CRF+). Minimal overlap in DE miRs was observed between tissues or between W0 and W12 resting timepoints (**Figure 4D**). Four were shared between muscle and exosomes at W0 and only one at W12. **Figure 4E** summarizes the miR profiles differentially responsive to acute exercise in fMQ+/CRF+ (vs. all others) at both W0 and W12. Across acute response time points (0h, 3h, 24h) at W0 and W12 HOSVD and subsequent downselection of features retained 447 DE miRs with 94 at W0 and 93 at W12 in muscle (39/94 and 55/93 higher in fMQ+/CRF+) and 131 at W0 and 129 at W12 in exosomes (55/131 and 39/129 higher in fMQ+/CRF+). KEGG pathways analysis was performed on high confidence target mRNAs (**Figure 4F and Table S3).** The resting and acute response profile of fMQ+/CRF+ (vs. all others) suggests differential regulation of several pathways central to stem cell cycle regulation (*e.g.*, Signaling pathways regulating pluripotency of stem cells, p53, Ras), autophagy, and apoptosis (**Figure 4F, Table S3**). Additionally, pathways that regulate processes favorable to positive physiologic adaptations were also altered, including blood flow, angiogenesis, endothelial function (e.g., relaxin, HIF-1, MAPK), and metabolism (PI3K-AKT, MAPK, FoxO, **Figure 4F, Table S3**).

Integration of DGE and HOSVD pipelines reveals nine miRs that may be central to exercise adaptability

To further our understanding of the miR-mediated modulation of individual adaptability to exercise training (*i.e.*, IRH) we compared the select miRs retained after strict down-selection processes in the HOSVD modeling framework to the DE miR signatures obtained through straightforward DE analysis of the miR data alone in the context of MCID attainment. We constricted this cross-comparison to: (i) 3h acute responses in the untrained state (W0); (ii) 3h acute responses in the trained state (W12); and (iii) resting expression profiles at W12 vs. W0 (i.e., training responses). A total of 168 unique miRs were identified by DGE analysis and 59 by HOSVD, with 9 common to both pipelines (**Figure 5A, Table S1**). Five of the

nine miRs have no known prior linkage to exercise (**Figure 5B**). The high confidence mRNA targets are largely unique to each of the nine miRs with only two target genes shared (BMI1, ERBB2) between two miRs (**Figure 5B**). Pathway analysis of these high confidence mRNA targets (**Figure 5C and Table S3**) showed enrichment in FoxO, JAK-STAT, HIF-1, TGF-β, and PI3-AKT signaling, along with stem cell regulation (among others).

DISCUSSION

Long-term exercise training is the only lifestyle choice to date that has consistently demonstrated an ability to improve function and health across multiple tissues and organ systems. While single mode exercise prescriptions (*e.g.,* MICT, HIIT or progressive RT) improve specific indices of physiological function and overall health with some cross-over, adaptations to combined training have received much less attention.

HITT vs. TRAD phenomic adaptations

We show here that a 3 d/wk HITT prescription combined with 2 d/wk high-intensity, short rest interval RT is as efficacious as a TRAD regimen despite being less than half the duration per session. HITT equaled TRAD for gains in aerobic power as measured by VO_2peak and both TRAD and HITT induced central and peripheral adaptations resulting in training-induced gains in VO_2peak. Interestingly, our findings suggest TRAD was advantageous for enhancing the mechanisms driving both O_2 pulse and capillary angiogenesis, while HITT more effectively induced biogenesis of IMF mitochondria, the pool of myofiber mitochondria typically resistant to exercise adaptation[33].

Even though the RT prescriptions in HITT and TRAD differed substantially in loading intensity (9 RM vs. 13 RM) and work/rest intervals, gains in strength and muscle power were generally comparable except for upper body strength gains which favored HITT. The nearly two times greater gain in anaerobic power among HITT compared to TRAD was not surprising given the principle of training specificity: the HITT prescription involved two Wingate-like 30s maximal power cycle sprints during each HITT session 3 days per week (*i.e.*, 2 of 10 HITT intervals each session). Although gains in total lean mass and limb lean mass

values did not differ by prescription, hypertrophy at the myofiber level was superior in TRAD and this advantage was associated with a more robust increase in the prevalence of Pax7^{+} SCs.

While a few phenotypic adaptations favored TRAD or HITT, the findings overall indicate the two prescriptions were similarly efficacious at inducing core health benefits with established clinical importance (*e.g.*, CRF, leg strength, muscle mass). It would be valuable to determine whether the peripheral adaptation advantages (e.g., myofiber hypertrophy and capillarization) seen here in TRAD result in continued, progressive gains or a divergence of performance adaptations over longer term training.

Detraining signature in muscle

After four weeks of detraining, indices of muscle mitochondrial capacity returned to baseline levels, in agreement with previous literature[34,35]. Training-induced gains in muscle capillarization remained after 4 weeks of detraining, consistent with prior work,[34] although others have reported partial reversal during a similar detraining period.[36] The detraining-induced reduction in the histological prevalence of Pax7+ muscle SCs is also consistent with previous studies in young[37] and older[38] adults. Though detraining leads to reversal it should not be assumed that the effects of exercise are lost. Previous work suggests that a “memory” signature exists in muscle stem cells that facilitates adaptation when exercise is resumed[39]. In older adults it has been shown that if exercise training is resumed following detraining, SC abundance may rebound even above the increase from the previous training period[38].

Interestingly, detraining myofiber atrophy occurred in an exercise prescription-specific manner. TRAD participants retained the training-induced hypertrophy noted for type II myofibers and mean fCSA, whereas HITT lost all gains in myofiber size. Myofiber hypertrophy, which occurs with endurance training,[40–42] especially with cycling[42,43] in untrained adults, appears to be retained during short-term detraining[44,45]. The preserved fCSA unique to TRAD may therefore have been linked to mechanisms unique to MICT and the cycling modality used. Detraining DE miRs in HITT mapped to 126 of the 354 mRNAs in the KEGG PI3K-AKT signaling pathway vs. only 12/354 for TRAD, suggesting downstream

mTOR-mediated protein synthesis signaling[46] was differentially impacted in HITT versus TRAD during detraining. Considering the typical inhibitory nature of miRs, this suggests greater suppression of protein synthesis in HITT, leading to the detraining atrophy seen in HITT but not TRAD.

Differentially expressed miRs across serum exosomes and muscle

Over 1,000 miRs have been linked to various exercise modalities, durations, intervals, intensities and sample types. (**Table S1** lists PMIDs linking miRs in this study to exercise with relevant sample types indicated. *The full manually curated list of exercise-responsive miR is available upon request*). Since the majority of exosomal miRs originate from vascular endothelial cells, platelets, lymphocytes and monocytes,[47] it follows that the miR signatures of the exercise response in serum exosomes and muscle would be largely independent. Consistent with this prediction and prior reports,[48,49] our observation that the serum exosomal miRs altered in response to exercise were mostly distinct from those altered by exercise in muscle implies that miR release from muscle is not a dominant contributor to subsequent changes in circulating miR levels.

We observed significant baseline (*i.e.*, pre-exercise) differences in the levels of 102 muscle-derived miR and 42 serum exosomal miRs between females and males (**Figure 2F**). This finding is in line with published reports indicating that the acute and chronic integrative molecular response to exercise differs between males and females.[50,51] Six of the miRs DE between males and females at baseline were found to be shared across muscle and exosomes (miR-15b-5p, 199a-3p, 199b-3p, 361-5p, 381-5p and miR-12116). All six were found to be DE in response to exercise in at least one of the comparisons (**Figure 2**). Since the study population overall and within HITT and TRAD was comprised of roughly equal numbers of males and females, all 6 are presumably exercise responsive miRs with “sexually dimorphic” expression.

We observed a robust DE response among serum exosomal miRs immediately post-exercise in both untrained and trained states while the DE response for muscle-derived miRs peaked 24h post-exercise. These response kinetics mirror previous reports indicating changes in serum exosomal miR expression

immediately after cycling exercise with a decline to baseline levels within 90 minutes of rest,[52] and an upregulation of muscle miRs peaking around 8h post-exercise.[53] The effects of single mode exercise interventions on muscle and exosomal miR levels have largely focused on the acute (i.e. <24h) response,[54–56] while the effects of extended training and/or detraining have been largely ignored. Of the 12 miRs associated with a 6-month detraining period in mice,[39] none linked to detraining in this trial. Our results suggest a much more potent miR response to detraining in muscle than in serum exosomes.

Multidimensional modeling and integration

The key purpose of employing HOSVD was to map biocircuits of IRH integrating both phenomic and miR signatures that converge on the fMQ+/CRF+ classification. The dominance of miR among the down-selected features (524 miR vs. 87 phenomic) is reflective of the overall numbers of input features (37,026 miR vs. 881 phenomic); not an indication of preferential importance for miRs. The existence of integrated circuits associated with MCID attainment (i.e., fMQ+/CRF+ vs. all others) is supported by the identification of LVs related to inflammation, angiogenesis, and adiposity. IL-6, which promotes cell senescence and tissue remodeling in healthy individuals[57] but is associated with disease and maladaptation when chronically elevated,[58] was lower in fMQ+/CRF+ individuals at baseline. There were also overlapping signatures between capillary supply and miR targeted pathways related to angiogenesis. HOSVD predicted changes in the PI3K/AKT pathway, a potent stimulator of angiogenesis and endothelial cell proliferation,[59,60] and HIF-1 signaling, a key regulator of angiogenesis and endothelial cell function[61] as well as stem cell function. Trunk fat, specifically android fat, was lower in fMQ+/CRF+ and there was greater android fat loss in fMQ+/CRF+ across training. FOXO signaling which is a key promoter of fat oxidation and mitochondrial lipid metabolism was differentially regulated in fMQ+/CRF+.[62] It is important to note that only 131/524 had strong evidence for miR/gene target interaction and were used for pathway analysis. Thus, much remains unknown about the pathways linked to fMQ+/CRF+ responder status.

Nine miRs linked to fMQ+/CRF+ are robust to methodological and sampling differences of DGE and HOSVD.

In addition to the mathematical differences in the DGE and HOSVD approaches, the pipelines differed in number of participants (80 in DGE analysis of MCID categories vs. 75 in HOSVD), miR data format (*i.e.,* individual timepoints in DGE versus change scores between timepoints in HOSVD) and inclusion of metadata (*i.e.* sample type only in DGE analysis by MCID, vs. extensive metadata use in HOSVD). The approach taken here serves as an illustration of the power of combining multi-dimensional models with standard DE pipelines as a means of prioritizing and identifying influential features. The fact that the same nine miRs appear in the output of both pipelines is evidence of the robustness of the association of these miRs with individual attainment of clinically important exercise-induced health benefits (e.g., fMQ and CRF).

Among the nine miRs, miR-656-3p and miR-3622-5p were linked to the acute exercise response in untrained individuals. miR-656-3p is downregulated in the plasma of female synchronized swimmers[63], promotes viability and migration of placental mesenchymal stem cells, and targets HIF-1alpha[64], suggesting a potential role in exercise-induced tissue hypoxia and angiogenesis. Although miR-3622b-5p has no reported link to exercise, it targets ERBB2 which plays a role in skeletal muscle repair and fibrosis in rats[65].

miR-589-5p and miR-95-3p had no previous link to exercise that we found acutely responsive to exercise in the trained state. miR-589-5p, which was upregulated in exosomes of the nonresponders in the trained state, is reported to reduce oxidative stress in human retinal microvascular endothelial cells via targeting EGR1[66], suggesting a possible response to oxidative stress in nonresponders. miR-95-3p has been shown to regulate cyclin-dependent kinase inhibitor 1A (CDKN1A), suggesting a role for miR-95-3p in the increased levels of CDKN1A reported to occur after exercise[67,68] and the cell proliferation / stem cell cycle regulatory responses to exercise.

The other five miRs in the group of nine were differentially expressed at rest from W0 to W12, suggesting

linkage to the differential exercise training adaptations separate from acute exercise responses. Of these, miR-935 and miR-12296-5p are previously unknown exercise-responsive miRs, with exosomal miR-935 upregulated in fMQ+/CRF+ and exosomal miR-338-5p downregulated in fMQ+/CRF+. Exosomal miR-935 has been shown to protect against oxidative stress in human cardiac progenitor cells[69]. miR-935 also targets NOTCH1, part of the NOTCH pathway shown to play a role in the beneficial effects of exercise on hippocampal neurogenesis and cognitive function in mice[70]. miR-338-5p targets NRP1, an angiogenic growth factor that is upregulated in response to exercise[71], suggesting a role for miR-338-5p in exercise-induced angiogenesis. It has also been shown to play a role in skeletal muscle in response to hypoxia[72] and inflammation and oxidative stress[73] in rats.

miR-1296-5p and miR-376a-5p were downregulated in muscle of fMQ+/CRF+ responders in response to training. Both have reported links to exercise, with a downregulation of miR-1296-5p in exosomes reported in response to fatiguing freestyle swimming[16], and an upregulation of miR-376a-5p in plasma reported in response to aerobic exercise training[74]. miR-376a-5p plays a role in the response to hypoxia and may promote cartilage repair by promoting proliferation and reducing apoptosis[75]. miR-181d-5p, previously reported to be downregulated in plasma of female synchronized swimmers[63], was downregulated in muscle of fMQ+/CRF+ in training and in exosomes in the acute training response. miR-181d-5p targets BCL2 and IRS2 and may thus play a role in apoptosis and insulin resistance. A recent report also implicates miR-181d-5p in reducing hypercholesterolemia by targeting PCSK9[76]. In mice, it reportedly also targets KLF6 to modulate apoptosis and inflammation in kidneys after IR injury[77]. NEAT1, a lncRNA shown to modulate the exercise-induced improvements in atherosclerosis[78], inhibits oxidative stress in human vascular endothelial cells by activating the miR-181-d-5p/CDKN3 axis[79].

Summary

In summary, both TRAD and HITT were highly efficacious combined exercise interventions that similarly improved physiological performance, clinically important health benefits and markers of skeletal muscle health and function despite their differences in intensity and session duration. Unique miR signatures

were identified across exercise doses, training status, and early-phase detraining for serum-derived exosomes and muscle, with additional differences noted due to biological sex. We implemented MCIDs to establish individual exercise responsiveness on two key health benefits and employed HOSVD machine learning to map biocircuitry associated with inter-individual response heterogeneity that integrated over 37,000 phenomic and molecular features followed by rigorous down-selection of key features. Cross-validation analysis of DGE and HOSVD yielded a core signature of nine miRs linked to exercise responsiveness. We believe the interrogation undertaken here provides advances in: (i) exercise dose-response physiology; (ii) orchestrated early-phase detraining responses; and (iii) the pursuit of mechanisms to explain inter-individual exercise response heterogeneity that may be leveraged in the future to optimize and individualize exercise prescriptions.

ADDITIONAL RESOURCES

This trial was registered at ClinicalTrials.gov (NCT03380923)

ACKNOWLEDGMENTS

We thank all the participants for their hard work and commitment to the trial. We also greatly appreciate the effort of study coordinators, interventionists and biospecimens collection and processing staff. This clinical trial was funded by a US Department of Defense Multidisciplinary University Research Initiative (MURI) awarded and administered via the Office of Naval Research under grant N000141613159. Figure 4 was created in part using Biorender (license available: *https://BioRender.com/a09x082)*

AUTHOR CONTRIBUTIONS

Conceptualization, TJB, MMB; **Methodology**, MMB, TJB, IA, JSM, KML, AM; **Software**, JSM, MPC, ZAG, KML, KP, AM; **Validation**, MMB, JSM, MPC, MK, YW; **Formal Analysis**, JSM, MC, GRC, MMB, ZAG, AM; **Investigation**, JSM, MPC, BP, SCT, RSS, KML, ZAG, ABS, SMO, SY, DJD, CJK, KP, MBB, JM, IA, YW, GM, GRC, SP, TJB, MK, MMB; **Resources**, TJB, MMB, MK; **Data Curation**, JSM, MPC,

CJK, SY, SMO, KML, BP, YW; **Writing – Original Draft**, JSM, MMB, MPC, ZAG; **Writing – Review & Editing**, JSM, MPC, BP, SCT, RSS, KML, ZAG, ABS, SMO, SY, DJD, CJK, KP, MBB, IA, YW, GM, GRC, SP, TJB, MK, MMB; **Visualization**, JSM, MPC, MMB, AM; **Supervision**, TJB, MK, MMB, SCT; **Project Administration**, SCT, ABS, TJB, MMB, MK; **Funding Acquisition**, TJB, MMB.

DECLARATION OF INTERESTS

The authors declare no competing interests.

Supplemental Information

Figures S1-S5, Table S2

Tables S1, S3 (Excel files containing additional data too large to fit in a PDF, related to figures 2 and 3).

FIGURE LEGENDS

Figure 1. Consort diagram (A) and participant characteristics (B).

Figure 2. miR signatures of exercise prescription, training status and sex are evident in serum exosomes and muscle.

(A-G) DE miR identified as $p \leq 0.05$, $|FC| \geq 1.5$ and minimum average read count of 10 reads in each category. Numbers above bars indicate the number of DE miR. Numbers to the right of the UpSet plots (A-C,F,G) indicate the total DE counts by category and shared between categories.

(A) UpSet plot showing miR differentially expressed (DE) in muscle in response to TRAD (n=43) or HITT (n=47). Comparisons of 3h and 24h at each W0 and W12 (vs. baseline W0 pre) are shown.

(B) UpSet plot comparing miR DE in exosomes in response to TRAD (n=43) or HITT (n=47). Comparisons of 0hr, 3h and 24h at W0 (left, vs. baseline W0 pre) and W12 (right, vs. baseline W12 pre) are shown.

(C) UpSet plot comparing DE miR part of the general response to exercise in muscle (left, n=90) and exosomes (right, n=90). Comparisons at the indicated timepoints at W0 and W12 (vs. corresponding pre baseline) are shown.

(D) DE miR at baseline between Females (n=48) and Males (n=42).

(E) UpSet plot showing miR DE in muscle in response exercise in Females (n=48) and Males (n=42). Comparisons of 3h and 24h at each W0 and W12 (vs. baseline W0 pre) are shown.

(F) UpSet plot comparing miR DE in exosomes in muscle in response exercise in Females (n=48) and Males (n=42). Comparisons of 0hr, 3h and 24h at W0 (left, vs. baseline W0 pre) and W12 (right, vs. baseline W12 pre) are shown.

(G) DE miR associated with detraining (W16 vs W12 pre) in muscle (n=89) and exosomes (n=89) for the overall response and for TRAD and HITT separately.

Figure 3. Wide inter-individual response heterogeneity in clinically important outcomes and linked miR signatures.

(A-B) Waterfall plots showing individual's % change in cardiorespiratory fitness (CRF) (A) and % change in functional muscle quality (fMQ) (B). (A-B) Individual responses are color coded for HITT and TRAD participants. Horizontal line is the minimum clinically important difference (MCID).

(C) Punnett square classification of participants who attained (+) or did not attain (-) MCID for fMQ and CRF.

(D-F) UpSet plots showing miR signatures of fMQ+/CRF+ dual responders (n=30) versus all others (n=50) in both muscle and exosomes. Differentially expressed (DE) miRs identified as $p \leq 0.05$, $|FC| \geq 1.5$ and minimum average read count of 10 reads per category. Numbers above bars indicate the number of DE miR. Numbers to the right of the UpSet plots (D-F) indicate the total DE counts by category and shared between categories. Target gene networks of DE miR identified in fMQ+/CRF+ responders in each panel show high-confidence mRNA targets regulated by at least 2 DE miR in the dataset. miR with red outlines have no known link to exercise. mRNA nodes with blue outlines are exercise-responsive mRNAs in MetaMEx.

(D) UpSet plots summarizing the numbers of DE miR 3h post-acute exercise in muscle (left) and exosomes (middle). The numbers of miRs DE at this acute response timepoint are shown for fMQ+/CRF+ dual responders vs. all other participants in both the untrained (W0) and trained (W12) states. W0 and W12 high confidence target gene networks of DE exosomal miR in fMQ+/CRF+ responders are shown on the right and available in the online NDEX library using the link provided in Table S2.

(E) UpSet plot showing DE miR associated with training (w12pre vs. w0pre) in muscle and exosomes. High confidence target gene networks of DE muscle miR in fMQ+/CRF+ responders linked to training are shown on the right and available in the online NDEX library using the link provided in Table S2.

(F) UpSet plot showing DE miR associated with detraining (w16rst vs. w12pre) in muscle and exosomes. High confidence target gene networks of DE muscle miR in fMQ+/CRF+ responders linked to detraining are shown on the right and available in the online NDEX library provided in Table S2.

Figure 4. Multidimensional biocircuitry linked to inter-individual response heterogeneity via higher order singular value decomposition (HOSVD).

(A) Punnett square displaying the observed distribution of minimum clinically important difference (MCID) scores for functional muscle quality (fMQ) and cardiorespiratory fitness (CRF); achieved MCID (+); did not achieve MCID (-). Distribution by sex is also shown.

(B) Categories of HOSVD input features to model biocircuitry of fMQ+/CRF+ dual responders vs. all others. The input features across these categories totaled 881 phenomic and 37,026 miR (including all timepoint contrasts in exosomes and muscle).

(C) Summary of key input features among the down-selected most influential top 5% of features from the HOSVD models of MCID classification fMQ+/CRF+ vs. all others.

(D) DiVenn plot of muscle and exosomal differentially expressed miRs (from top 5% of HOSVD features) in fMQ+/CRF+ vs. all others in fasted, morning resting samples (prior to the acute exercise bout) in the untrained state (W0) and trained state (W12). Red = upregulated, blue = downregulated, and yellow = miR shared across nodes that are upregulated in one node and down in another.

(E) DiVenn plot of muscle and exosomal differentially expressed miRs (from top 5% of HOSVD features) in fMQ+/CRF+ vs. all others collapsed across the acute exercise response time points for serum exosomes (0h, 3h, 24h) and for muscle (3h, 24h). Red = upregulated, blue = downregulated, and yellow = miR shared across nodes that are upregulated in one node and down in another. Acute response miRs were determined as change from pre-exercise within the given acute response bout (i.e., untrained W0 or trained W12).

(F) KEGG 2021 top 20 non-disease enriched pathways ($p \leq 0.05$) resulting from downselection of the differentially expressed pre-exercise and acute response miRs at W0 and W12 in serum exosomes and muscle with high confidence (strong evidence) mRNA targets.

Figure 5. Cross-validation of miRs linked to inter-individual response heterogeneity.

For this cross-validation we constricted the analysis to: (i) 3h acute responses in the untrained state (W0); (ii) 3h acute responses in the trained state (W12); and (iii) resting expression profiles at W12 vs. W0 (i.e., training responses).

(A) Venn diagram showing the subsets of miR resulting from these constricted analyses which equaled 168 unique miRs identified using differential gene expression (DGE) analysis of miR data alone, and 59 miRs from the top 5% of HOSVD features with nine common to both pipelines; featured in the table. Five of the nine miRs (indicated by red text) have no known prior linkage to exercise.

(B) Target gene networks of DE miR in fMQ+/CRF+ responders generated from the nine miRs common to both DE and HSOVD pipelines after filtering to only high-confidence mRNA targets. miRs with red outlines are miRs with no known link to exercise. mRNA nodes with blue outlines are exercise-responsive mRNA in MetaMEx.

(C) KEGG 2021 top 20 non-disease enriched pathways ($p \leq 0.05$) of the high-confidence mRNA targets from panel B.

Table Legends

Table 1. *In vivo* physiological and performance adaptations to HITT and TRAD exercise training. VO_2peak: peak oxygen consumption; RER: respiratory exchange ratio; 1RM: one repetition maximum; MVIC: maximal voluntary isometric contraction; bt/min: beats per minute; W: watts; N*m: newton meters;

Table 2. *Ex vivo* skeletal muscle adaptations to HITT and TRAD exercise training and detraining. Cap, capillary; SCs, satellite cells; CS, citrate synthase; SS, subsarcolemmal mitochondria; IMF, intermyofibrillar mitochondria; cx, complex, IFN-**γ**, Interferon gamma; IL, Interleukin, TNF-α Tumor Necrosis Factor alpha. For post-hoc contrasts, symbols on the variable name localize time effects detected in the full cohort, whereas the same symbols on time points within HITT or TRAD localize the same time effects within group: *change pre-training to post-training, $p < 0.05$; †change post-training to detraining, $p < 0.05$.

STAR METHODS

Key resources table

REAGENT or RESOURCE	SOURCE	IDENTIFIER
Antibodies		
Myosin Heavy Chain I (mouse IgG2b)	Developmental Studies Hybridoma Bank	BA-D5
Myosin Heavy Chain IIa (mouse IgG1)	Developmental Studies Hybridoma Bank	A4.74s
PAX7+ (mouse IgG)	Developmental Studies Hybridoma Bank	PAX7
Laminin (rat IgG)	ThermoFisher	MA1-06100
Ulex Europaeus Agglutinin I (UEA-1)	Vector Labs	L-1060
AlexaFluor 488 secondary (anti-mouse IgG2b)	ThermoFisher	A-21145
AlexaFluor 488 tyramide SuperBoost Kit, streptavidin	ThermoFisher	B40932
AlexaFluor 594 secondary (anti-mouse IgG1)	ThermoFisher	A-21121
AlexaFluor 647 secondary (anti-rat IgG)	ThermoFisher	A-21247
Biotin-conjugated goat anti-mouse secondary	Jackson ImmunoResearch	115-065-003
Chemicals and reagents		
VectaShield mounting media with DAPI	Vector Labs	H-1200-10
1x PBS (pH 7.4)	Fisher Scientific	BP243820
Gibco Goat serum	Fisher Scientific	PCN5000
2.5% Normal Horse Serum	Vector Labs	S201250
Critical commercial assays		
MSD V-Plex Pro-Inflammatory Panel 1	MesoScale Discovery	K15049D
Testosterone Tosoh AIA automated immunoassay	TOSOH Bioscience	025204
Dehydroepiandrosterone (DHEA) Tosoh AIA automated immunoassay	TOSOH Bioscience	025222
Sex-hormone binding globulin Tosoh AIA automated immunoassay	TOSOH Bioscience	025239
Androstenedione Tosoh AIA automated immunoassay	TOSOH Bioscience	025221
Human FGF-21 ELISA	Millipore	EZHFGF21-19K
IGF-1 ELISA	ALPCO	22-IGFHU-E01
IGFBP-3 ELISA	ALPCO	22-BP3HU-E01
miRVana Paris Kit (muscle total RNA isolation)	ThermoFisher	AM1556
Total exosome isolation and Exosome RNA/Protein Isolation Kit	Life Technologies	4478545
Agilent 2100 Bioanalyze DNA1000 chip	Agilent	5067-4626

Ion P1 chip v3 with Ion PI Seq 200 kit v3	Life Technologies	4488315
Deposited data		
miR fastq/read matrices	Gene Expression Omnibus	GSE269533
Software and algorithms		
Partek Flow v12.0	Partek	N/A
R	R Development Core Team	www.r-project.org
R Package: Targets[80]	Targets	https://cran.r-project.org/web/packages/targets/index.html
R Package: Tidyverse[81]	Tidyverse	https://cloud.r-project.org/web/packages/tidyverse/index.html
R Package: lme4[82]	lme4	https://cran.r-project.org/web/packages/lme4/index.html
R Package: ez[83]	ez	https://cran.r-project.org/web/packages/ez/ez.pdf
Limma	Bioconductor	https://bioconductor.org/packages/release/bioc/html/limma.html
Other		
Ensure Plus liquid protein supplement (8 oz)	Abbott Labs	64905

RESOURCE AVAILABILITY

Lead Contact

Marcas Bamman (mbamman@ihmc.org) is the lead contact for this manuscript and should be contacted for further information and requests for resources and reagents.

Materials availability

No unique reagents or materials were generated in these studies.

Data and code availability

Raw small RNA-Seq data for all muscle and exosome miR analysis have been deposited in the Gene Expression Omnibus (GEO) database [GSE269533] and are publicly available as of the date of

publication.

Any additional information required to reanalyze the data reported in this paper is available from the lead contact upon request.

EXPERIMENTAL MODEL AND STUDY PARTICIPANT DETAILS

Trial Design

This trial was a parallel, randomized, two-arm, exercise dose-response efficacy trial to investigate acute molecular responses and training adaptations to two distinct prescriptions of combined exercise training in young adults. The overall trial design is summarized at ClinicalTrials.gov under the protocol identifier NCT03380923 and summarized graphically in **Figure S1**. The protocol was 16 weeks in duration and divided into two phases: 1) a 12-week progressive exercise training phase with 3 training sessions per week; and 2) a 4-week detraining phase immediately following the training phase. *In vivo* physical performance and physiological phenotyping were performed pre- and post-training while *ex vivo* tissue and molecular phenotyping were performed pre- and post-training and then again following the 4-week detraining phase. Acute exercise response studies for molecular profiling of serially collected biospecimens occurred in both the untrained (pre) and trained (post) states.

Recruitment, Enrollment, Randomization

The Precision High-Intensity Training Through Epigenetics (PHITE) trial was approved by the University of Alabama at Birmingham (UAB) Institutional Review Board for Human Use (Protocol: F160512012), was conducted in accordance with the Declaration of Helsinki, and is registered in ClinicalTrials.gov (NCT03380923). Healthy, young adult female and male civilians aged 18-27 years were recruited from the greater Birmingham, Alabama catchment area. Participant recruitment began in February 2017 with all human participant intervention sessions and testing completed by July 2021. All participants completed health, physical activity, and medical history questionnaires during screening. Participants were exercise-naïve (*i.e.*, no history of regular exercise training in the past 12 months) but could tolerate exercise without onset of angina/ischemia. Participants were excluded due to: current pregnancy, body

mass index (BMI) ≥ 30, lidocaine allergy, diabetes, uncontrolled hypertension or other vascular disease, musculoskeletal disease, mental health disorders, or any other chronic or infectious disease that would preclude participation. Each volunteer provided written, informed consent prior to participation. All screening, enrollment/randomization, testing, exercise training, and biospecimen collections were completed at the UAB Center for Exercise Medicine (UCEM) in Birmingham, Alabama.

After pre-screening, informed consent and screening, participants completed the US Marine Corps' Initial Strength Test (IST), Multi-dimensional Aptitude Battery II (MABII) cognitive performance test and other baseline testing, followed by randomization to a traditional combined exercise prescription (TRAD) or military-relevant high-intensity tactical training prescription (HITT), as described in detail below. Randomization to TRAD or HITT was stratified by sex (assigned at birth) to attain sex balance and enable sex as a biological variable to serve as a valuable input feature into modeling of inter-individual response heterogeneity. We did not hypothesize nor power the trial to test any groupwise differences in responsiveness between females and males and, given similar distributions of the two sexes (assigned at birth) in the four responder classifications (**Figure 4A**), the effect(s) of sex on intervention adaptations appeared to be minimal. We did, however, summarize sex differences in baseline phenotype (**Figure 1B**). A CONSORT diagram summarizing recruitment, enrollment, and retention across the phases of the trial is presented in **Figure 1A**.

METHOD DETAILS

Familiarization and Exercise Training

Prior to the first acute response exercise bout and subsequent exercise training, participants underwent three familiarization sessions to establish proper exercise technique and quality of movement and to progress volume and intensity to mitigate muscle soreness/damage/inflammation as sessions progressed to the higher intensity resistance training. The first full volume and intensity bout was the acute response testing bout described below. Participants then completed 12 weeks of supervised, progressive, combined exercise training.

<u>TRAD:</u> Participants randomized to TRAD completed 30 min of steady-state, moderate intensity

continuous exercise training (MICT) 3x/week (M, W, F) at a target of 70% heart rate reserve (HRR) using a LifeFitness 95CE Discover SE cycle ergometer or LifeFitness 95T Discover SE treadmill. HRR was defined by resting HR and peak HR determined during the baseline VO_{2peak} test. The use of both stationary cycle and treadmill provided variety with cycling performed 2x/wk and treadmill 1x/wk. Twice per week (M, F), this MICT was followed by moderate intensity whole-body resistance exercise training. Volume and intensity were prescribed as 3 sets per movement with loads targeting 13-repetition maximum (13RM) across nine movements: (chest press, seated row, overhead press, lat pulldown, triceps extension, biceps curl, calf press, squat or leg press, knee extension) plus 3 sets of abdominal crunches to volitional fatigue. Both groups performed squats on Monday and leg press on Friday to introduce variety. Sets were separated by ~60 sec rest. To ensure prescription standardization, intensity was monitored closely and progression occurred regularly. For MICT, workloads on the stationary cycle and treadmill were increased as needed to maintain 70% HRR. For resistance training, external loads were increased as needed to maintain 11-15RM, targeting 13RM. The TRAD combined exercise bout duration (M, F) was ~90 min while the MICT-only session each W was completed in ~40 min.

HITT: In lieu of MICT for endurance exercise, the HITT prescription focused on explosive movements and sustained near-maximal to maximal power during 30-sec intervals. Participants randomized to HITT completed a 10-round circuit of nine movements performed 3x/week (M, W, F): rowing sprint, box jumps, burpees, split squat jumps, kettlebell swings, cycling sprints, battle ropes, wall balls, and dips each for 30 sec at maximal effort, separated by 30 sec of rest. The 30-sec cycling sprint was performed twice in the 10-round circuit. Matching TRAD for combined training, the HITT prescription included resistance training twice per week (M, F) executing the same movements as TRAD. There were three major differences in the resistance training prescription for HITT: (i) loading intensity was higher (9RM vs. 13RM); (ii) movements were performed as “supersets” with two movements recruiting antagonistic or unaffected muscle groups completed in succession with no rest (e.g., chest press and seated row); and (iii) rest intervals between sets (specifically, between supersets) were only 30 sec. To ensure prescription standardization, intensity was monitored closely, and progression occurred regularly. For the explosive

10-round circuit, maximal intensity was strongly encouraged throughout; thus, progression was accomplished by maximizing power output (rowing sprint, cycling sprints) or repetition counts (all other movements) accomplished in each 30-sec interval. For the resistance training component of HITT, external loads were increased as needed to maintain 8-10RM, targeting 9RM. The HITT combined exercise bout duration (M, F) was ~45 minutes while the HITT-only session each W was completed in ~15 min.

Participant Adherence

Session adherence rates for the 12 weeks of 3x/wk training were high with an overall adherence of 94% ± 5% attendance (TRAD: 93.7% ± 5.3%; HITT: 94.3% ± 5.7%). The 70% HRR target intensity for the MICT component of TRAD across the 12 wk of training was achieved, averaging 70.2% ± 5.1% HRR. There was no comparable heart rate-defined intensity target for the HITT intervals, as intensity was maximum and not steady state. For the progressive RT component of each program, prescribed loading intensity was 8-10 repetitions maximum (RM) per set for HITT, and lower at 11-15 RM for TRAD. These intensities were met as exemplified by representative lower and upper body movements: squat (HITT 9.8 ± 2.1; TRAD 12.9 ± 2.3 rep/set) and chest press (HITT 9.1 ± 2.4; TRAD 11.8 ± 3.0 rep/set). Under the direct supervision of the interventionist, participants also adhered to the differentially prescribed between-set rest intervals in HITT vs TRAD, whereby HITT were given only 30 s between supersets (2 sequential movements with no rest) vs. protracted rest periods of 60 s between individual sets for TRAD (with no supersets).

Acute Response Studies

Prior to and at the conclusion of the 12-week training program, participants completed an acute response exercise bout with serial biospecimen collections to map acute and longer-term molecular responses to TRAD vs. HITT. Acute response studies were standardized pre- and post-training; performed in the morning fasted state (8-10 hour fast) between 0600 and 0900, targeting a start time 0630-0730 to minimize any potential influences of each individual's circadian clock. For females, the phase of the menstrual cycle was recorded leading into the pre-training acute response bout and used to schedule

the post-training acute response bout to standardize the phase of the menstrual cycle within each participant across the two acute bouts. Standardizing the menstrual phase among all female participants was deemed not feasible.

Each acute response study began by verifying the fasting state and abstinence of exercise over the previous 48 h, completing the ASA24 24h dietary recall, and collecting data on sleep quality the previous night. To recapitulate the 24h nutritional state leading into each acute response bout, in preparation for the post-training acute bout each participant was encouraged to consume the same 24h diet recorded at the pre-training acute bout. A supine rest period of 15 minutes was followed by resting blood and muscle collections. The supervised bout of combinatorial (M, F prescription) TRAD or HITT was then performed. Post-exercise blood draws were conducted as follows: immediately (within 10 min), 3h, and 24h post-exercise. Post-exercise muscle biopsies were performed 3h and 24h post-exercise. The per protocol accepted windows for post-exercise biospecimen collections were ± 15 min at 3h and ± 2 h at 24h. Participants consumed a standardized nutrition shake after the immediate post-exercise blood draw. The shake was commercially available (Ensure Plus, 64905) including an alternative for those who were on a vegan diet or lactose intolerant (Ensure 67453). No additional calories were consumed and participants rested (other than limited walking) prior to the 3h post-exercise biospecimen collections. Participants returned in the morning fasted state for 24h post-exercise blood and muscle collections.

Detraining

At the conclusion of training and the battery of post-training tests, participants were instructed to continue normal activities of daily living but to abstain from organized or structured exercise for four weeks. Participants then returned for final biospecimen (muscle and blood) collection, in the morning fasted state, at the end of the four-week detraining period.

Clinical and Performance Phenotyping

Multidimensional Aptitude Battery-II (MAB-II): As part of baseline testing, the MAB-II was administered using Sigma Assessment Systems (Sigma Inc., Port Huron, MI, USA) to evaluate aptitude/intelligence. MAB-II uses ten domains (information, comprehension, arithmetic, similarities, vocabulary, digit symbol,

picture completion, spatial, picture arrangement, object assembly) to score verbal, performance, and full-scale IQ. Each domain consists of a 7-min timed test. The battery was administered in a quiet, private office using default software settings.

Body composition: Body composition was assessed via dual-energy x-ray absorptiometry (DXA) using a GE Lunar iDXA (GE Healthcare, Chicago, IL, USA) pre- and post-training. Total body scans occurred at least 24h prior to or after exposure to exercise and after a minimum 2h fast. All scans were analyzed using GE Encore software v18 which yielded over 300 dependent variables. The primary variables of interest were total body fat, visceral adipose tissue, subcutaneous abdominal adipose tissue, body fat percentage, total lean mass, bilateral thigh lean mass, and bilateral arm lean mass.

Aerobic power (VO_2peak): VO_2peak was determined pre- and post-training using a continuous ramp protocol on a LODE Excalibur Sport (LODE B.V., Groningen, NL) cycle ergometer with sex-specific progression. For females, initial resistance was 50 W with an increase of 8.3 W/min for the first 9 min. This resistance increased to 15 W/min for the remainder of the test. For males, initial resistance was 75 W with an increase of 8.3 W/min for the first 9 min and then 25 W/min thereafter. Heart rate (HR) was measured continuously with a 3-lead ECG. Blood pressure was collected every other minute (all even minutes) while rating of perceived exertion (RPE) was collected every other minute starting 1 min after the start of the test (all odd minutes). The test was terminated when the participant reached volitional fatigue or was unable to maintain a cadence above 60 RPM. The main VO_2peak achievement criteria were volitional fatigue and achieving a respiratory exchange ratio (RER) > 1.10. The minimum RER attained across all W0 and W12 VO_2peak tests was 1.12 and the mean was 1.29. The main dependent variables of interest included absolute VO_2peak (L/min), relative VO_2peak (ml/kg/min), peak RER, peak HR, peak RPE, peak power (W), relative peak power (W/kg), and peak O_2 pulse.

Anaerobic power: Anaerobic power and fatigue resistance were measured using the standardized 30 s Wingate cycle test on either a LODE Excalibur Sport (LODE B.V., Groningen, NL) or Monark (Monark Exercise, Vansbro, SE) cycle ergometer pre- and post-training. Participants performed a 5 min warm-up with no load prior to the test. Per standard protocol, males were tested at a resistance of 0.7 kiloponds

per kilogram bodyweight and females were tested at a resistance of 0.67 kiloponds per kilogram. The dependent variables of interest included absolute (W) and relative (bodyweight adjusted, W/kg) peak and average power, along with rate of fatigue.

One-repetition maximum (1RM) strength testing: 1RM was assessed pre- and post-training. Participants warmed up on a cycle ergometer for at least 5 min prior to 1RM testing. The order of movements for testing was standardized to reduce muscle fatigue in agonistic movements and optimize recovery between 1RM tests. 1RM was determined for chest press, back squat, lat pulldown, knee extension, and overhead press. For each movement participants performed 8-12 reps with a light load, 3-5 repetitions with a moderate load, 2-3 reps with a moderately heavy load, then proceeded to 1RM testing. There were 1-2 min rest intervals between warmup sets and 2 minutes between 1RM attempts. 1RM was defined as the heaviest load lifted through a full range of motion preceding two failed attempts.

Knee extensor isometric strength and power: Peak unilateral maximum voluntary isometric contraction (MVIC) strength and dynamic power were evaluated on the dominant leg pre- and post-training using a Biodex System 4 Pro dynamometer (Biodex Inc., Shirley, NY, USA). To determine MVIC, three 5-s maximal knee extension contractions were performed at a fixed joint angle of 60˚. The three attempts were separated by 60 s rest. MVIC was defined as the peak torque generated during these contractions. Peak knee extension power was determined against a constant external resistance set at 40% of the MVIC torque. Participants completed five consecutive, full range of motion unilateral repetitions as rapidly as possible during the concentric phase (followed by a submaximal eccentric phase back to the starting position). Staff encouraged maximum effort throughout all repetitions. Peak concentric power of each repetition was extracted. Peak power was then defined as the highest power output achieved across the five concentric repetitions while average power was defined as the average of the five power peaks.

Counter movement jump (CMJ): The CMJ test was conducted to assess lower body explosive power based on maximum jump height pre- and post-training using AMTI Optima force plates (AMTI, Watertown, MA, USA). Participants warmed up on a cycle ergometer then completed two practice jumps followed by three maximal effort jumps. Participants were instructed by staff to squat and drive upward

as explosively as possible. Jump height was determined from hang time (i.e., time interval with zero force plate load between takeoff and onset of landing). The highest jump height attained over the three test repetitions defined peak performance score.

U.S. Marine Corps Initial Strength Test (IST): The IST was administered pre- and post-training. The IST consists of the following three tests performed in this specific order: (i) number of successful abdominal crunches in 2 minutes; (ii) number of successful pull ups in 2 min; and (iii) time to complete a 1.5-mile run. Participants underwent a supervised treadmill warmup for 10 min. and were instructed on proper technique and evaluation criteria for abdominal crunches and pull ups. The 1.5-mile run was conducted on a Life Fitness Elevation Series Treadmill (Life Fitness, INC, Rosemont, IL, USA) at 1% grade. Participants were encouraged to complete the test as quickly as attainable and were allowed to adjust the speed as needed until the 1.5-mile distance was completed. Results from each assessment were scored by current Marine Corps IST standards.

Biospecimen Collection and Processing

Blood: Blood samples were collected via standard venipuncture of an antecubital vein. A total of nine blood draws were performed per participant at timepoints as indicated in **Figure S1**. The pre- and post-training acute response bouts each included four blood draws: (i) fasted morning resting; (ii) immediately (within 10 min post-exercise; (iii) 3h post-exercise; (iv) 24h post-exercise. The ninth blood draw occurred after 4 wk of detraining in the fasted morning resting state. All draws included vacutainers to yield whole blood, serum, plasma cell-free DNA (Streck), and peripheral blood mononuclear cells (PBMCs via CPT).

Skeletal muscle biopsies: A total of seven *vastus lateralis* skeletal muscle biopsies were performed per participant as shown in **Figure S1** using our well-established protocol. The pre- and post-training acute response bouts each included three muscle biopsies: (i) fasted morning resting; (ii) 3h post-exercise; (iii) 24h post-exercise. The seventh biopsy occurred after 4 wk of detraining in the fasted morning resting state. Briefly, specimens were obtained under local anesthesia with 1% or 2% lidocaine using a 5 mm Bergström biopsy needle under suction. The incision was closed with a single stitch. After the pre-acute exercise biopsies, the thigh was wrapped in a pressure bandage during TRAD and HITT acute response

bouts. The seven serial muscle biopsies were performed by alternating thighs each subsequent biopsy. This has been our standard practice when the stimulus (whether acute response or long-term training) is equally bilateral. Repeated biopsy sites on each thigh were 1-2cm proximal to the previous biopsy site. The technique yields ~200-350mg of tissue which was quickly cleared of any visible fat and connective tissue. Muscle tissue was rapidly weighed, divided into 20-30mg aliquots, and snap frozen in liquid nitrogen. At biopsies 1, 4, and 7 (the three fasted, morning samples), approximately 50 mg were set aside and subsequently prepared for immunohistology. This sample was oriented cross-sectionally and mounted on cork in a mixture of tragacanth gum and optimal cutting temperature (OCT) compound. The mount was then frozen in liquid nitrogen-cooled isopentane for ~60 s. All muscle samples were then stored at -80˚C until analysis. In a subset of participants, approximately 50mg were set aside and processed in culture for isolation of muscle stem (satellite) cells for future experiments.

Serum Hormone and Cytokine Analyses

Systemic cytokine levels: To assess the potential effects of TRAD or HITT on systemic inflammation, circulating cytokine concentrations were determined in fasted, morning serum samples at baseline and post-training with the 7-plex MSD V-Plex Proinflammatory Panel I multiplex kit (MesoScale Discovery, Rockville, MD) using a MESO SECTOR S 600 according to manufacturer's guidelines (Rockville, MD) as we previously described[84]. The 7-plex cytokine profile includes: interferon gamma (IFN-y), interleukin (IL)-10, IL-12 p70, IL-1β, IL-6, IL-8, and tumor necrosis factor-alpha (TNF-α). All serum samples were analyzed across three plate assays with the two timepoints per participant analyzed on the same plate. Minimum assay sensitivities for each cytokine across the three plates were: IFN-y, 0.27 – 0.42 pg/mL; IL-10, 0.025 – 0.07 pg/mL, IL-12 p70, 0.07 – 0.17 pg/mL; IL-1β, 0.028 – 0.06 pg/mL; IL-6, 0.05 – 0.20 pg/mL; IL-8, 0.03 – 0.06 pg/mL; and TNF-α, 0.12 – 0.32 pg/mL. Where values were below detectable limits, the values were removed. Intra-assay and inter-assay CV% averaged, respectively: IFN-y, 3.84%, 8.62%; IL-10, 3.37%, 7.91%, IL-12 p70, 16.09%, 6.53%; IL-1β, 47.32%, 1.17%; IL-6, 7.91%, 3.92%; IL-8, 3.76%, 7.49%; and TNF-α, 3.92%, 12.09%. IL-1β was not analyzed statistically because 75% of the values were below detectable limits.

Anabolic hormone and growth factor profiles: As part of baseline phenotype profiling, a targeted panel of anabolic hormones and growth factors were assayed in fasted, morning serum samples. Total testosterone (total T), androstenedione, dehydroepiandrosterone sulfate (DHEA-S), and sex hormone binding globulin (SHBG) were measured on a TOSOH Bioscience AIA900 (South San Francisco, CA). Fibroblast growth factor (FGF)-21 (Millipore, Billerica, MA), insulin-like growth factor (IGF)-1 (ALPCO, Salem, NH) and IGF binding protein (BP)-3 (ALPCO) were measured using single-target ELISA kits as we previously described.[85] All serum samples were across two assay runs per target. Minimum assay sensitivities across the two runs averaged: total T, 10 ng/dL; DHEA-S, 4.48 µg/dL; SHBG, 0.1 nmol/L; IGF-I, 23 ng/mL; IGFBP-3, 101 ng/mL; FGF-21, 31 pg/mL; and androstenedione, 0.1 ng/mL. Intra-assay CV% averaged: total T, 6.92%; DHEA-S, 7.10%; SHBG, 6.17%; IGF-I, 5.5%; IGFBP-3, 2.93%; FGF-21, 2.68% and androstenedione, 3.84%.

Skeletal Muscle Histology

General histology methods: Immunohistological protocols were performed on fasted morning biopsies collected pre-training, post-training and after detraining. For all immunostains, 6 µm sections were prepared via a cryostat microtome (Leica, Buffalo Grove, IL) at approximately -22˚C and stored at -80˚C until staining. Separate sections were cut to determine: 1) myofiber type distribution and type-specific cross-sectional area (CSA); 2) capillary density, capillary contacts per type I myofiber, and capillary contacts per type 2 myofiber; and 3) number of Pax7+ satellite cells (SCs) per 100 type I and 100 type II myofibers using our well-established protocols.[86–89] For each protocol, all time points within a given participant were immunostained and imaged together to ensure all steps and reagents including antibody concentrations, incubation times, image capture protocols, etc. were standardized.

Myofiber typing via myosin heavy chain (MHC) isoform immunohistochemistry: Our well-established protocol enables quantitation of MHCI, MHCIIa, MHCIIx/IIax and MHCI/IIa myofibers[90]. Stored slides were thawed in a humidity chamber at 37 ˚C for 10 min then rehydrated with 2 x 5 min incubations in PBS. After fixation in 1:1 acetone-methanol for 3 min, sections were washed 2 x 5 min in PBS and blocked with 5% goat serum in PBS for 20 min at room temperature. Primary antibodies against MHCI [0.9 µg/ml

BA-D5; Developmental Studies Hybridoma Bank (DSHB), University of Iowa, Iowa City, IA], MHCIIa (1.5 µg/ml A4.74; DSHB), and laminin (5 µg/mL, MA1-06100; ThermoFisher) were co-incubated for 30 min at RT. Sections were washed 3 x 5 min in PBS then incubated for 30 min at 37 ˚C with fluorophore-conjugated secondary antibodies to reveal anti-MHCI [Alexa Fluor 594 goat anti-mouse. 10 µg/mL, A-21145; ThermoFisher Scientific, Waltham, MA)], anti-MHCIIa [Alexa Fluor 488 goat anti-mouse, 5 µg/mL, A-21121; ThermoFisher)] and anti-laminin [Alexa Fluor 647 goat anti-rat, 5 µg/mL, A-21247; ThermoFisher)]. After a final 3 x 5 min PBS wash, sections were DNA counter-stained with DAPI-containing mounting media (VectaShield), then a cover slip was placed over the section, sealed with acrylic paint, then imaged.

Capillary histochemistry: Cryosections were stained for capillaries using the fluorophore-conjugated ulex europaeus agglutin-1 (UEA-1 1:100, FL1061-FITC conjugate, Vector Laboratories, Burlingame, CA), which binds to glycoprotein residues on the surface of vascular endothelial cells. Frozen sections were rehydrated, fixed, and blocked as described above. Sections were first stained using a MHC I and laminin cocktail for 90 min at room temperature using the methods above, washed 3 x 5 min in PBS, then incubated for 60 min with a secondary antibody cocktail containing AlexaFluor 594 (anti-MHC1), AlexaFluor 647 (anti-laminin), and UEA-I. Sections where washed 3 x 5 min in PBS then cover-slipped with DAPI-containing mounting media (VectaShield) and stored protected from light until imaged.

Pax7+ muscle stem (satellite) cell immunohistochemistry: Frozen cryosections were rehydrated and fixed as described above. Sections were then blocked from endogenous peroxidases with 3 x 150 µl drops of 3.0% hydrogen peroxide in PBS from the SuperBoost kit (Invitrogen) for 10 min at room temperature. Sections were washed 3 x 3 min in PBS then blocked in 2.5% horse serum for 60 min at room temperature. Following another 3 x 3 min wash in PBS, sections were incubated with 200 µl of 1:100 Pax7+ primary antibody (Developmental Studies Hybridoma Bank, cat#: PAX7) in 2.5% horse serum overnight at 4 ˚C. The following morning sections were washed 3 x 5 min in PBS, incubated in 1:1000 secondary antibody (biotinylated goat anti-mouse; Jackson ImmunoResearch) in 2.5% horse serum for 60 min at room temperature, then washed 3 x 5 min in PBS. Sections were then incubated at 1:100 v:v

1x HRP-conjugated streptavidin in PBS from SuperBoost kit for 60 min at RT, washed 3 x 5 min in PBS, then had its signal amplified with an incubation of 1:300 Alexa Fluor 488 tyramide reagent in amplification buffer (SuperBoost). After a 3 x 5 min wash, samples were re-blocked in 5% goat serum in PBS for 20 min at room temperature, then incubated in laminin and MHC I antibodies as described above. After staining, sections were slip covered, sealed, then stored at -20˚C in the dark until imaging.

Image analysis: All images were captured with a fluorescence microscope (BX51; Olympus, Tokyo, Japan) at 20x magnification with an XM10 camera (Olympus) using automated image stitching using CellSens Dimension (Olympus) to create a single high-resolution image of the complete mount. Myofiber type and fCSA were assessed using MyoVision[91] with the following parameters: fiber circularity > 0.50, fCSA range of 800-25,000 μm^2, and removal of peripheral edge fibers by moving the detected border of the entire tissue cross-section inward 30 µm. Capillary and Pax7+ satellite cell counts were performed manually by blinded laboratory staff using Image Pro 9 (Media Cybernetics, Rockville, MD).

Skeletal Muscle Mitochondrial Function Assays

Mitochondrial fractionation: Subsarcolemmal (SS) and intermyofibrillar (IMF) mitochondria were isolated using a modification of Rasmussen *et. al.*[92]. Snap-frozen muscle samples from fasted morning biopsies collected pre-training, post-training and after detraining (30-50 mg) were pulverized by hand using a liquid nitrogen-cooled mortar and pestle then homogenized in a 20:1 volume-to-weight solution of ice-cold Chappell-Perry isolation buffer (100 mM KCl, 50 mM Tris-HCl, 1 mM Na-ATP, 5 mM MgSO4, 0.1 mM EGTA, 0.2% BSA, pH 7.4) + protease inhibitor cocktail (CPRoche, mini-complete; CP+PIC). Homogenization was done at 990 rpm at 4˚C using a customized Wheaton mortar and pestle and recirculating cooling system. SS were isolated by centrifuging the muscle homogenate at 600 g for 10 min a 4˚C (Spin 1) then transferring the supernatant to a separate ice-cold tube for further centrifugation at 10,000 x g for 10 min at 4˚C (Spin 2) to yield the SS pellet. To maximize SS mitochondrial quantity, the pellet from Spin 1 was re-homogenized with the supernatant from Spin 2, after which Spins 1 and 2 were repeated. The supernatant was removed and saved for IMF isolation and the SS-enriched pellets obtained from both rounds of homogenization were resuspended with 30-50 µl CP+PIC and used

immediately or stored at −80˚C. The remaining supernatant was combined with the pellet from Spin 1 and a protease (*Bacillus* sp. Type XXVII, Sigma-Aldrich) was added to release the IMF fraction. Samples were re-homogenized then centrifuged using the parameters of Spin 2. The IMF mitochondrial enriched pellet was resuspended with 30-50 µl CP+PIC and used immediately or stored at -80°C.

Mitochondrial enzyme activity assays: SS and IMF mitochondrial enzyme activities were measured as we have described.[93] In brief, prior to assessment of mitochondrial complex activities, protein concentration was determined using a Lowry assay in duplicate. Complex I activity was immediately measured on a DU800 spectrophotometer using 2,6-dichloroindophenol (DCIP) at 600 nm. Complex IV activity was measured by the oxidation of cytochrome c at 550 nm. Complex I and IV data are represented as the pseudo first order rate constant (k) divided by protein concentration. Citrate synthase (CS) was measured as a surrogate index of mitochondrial volume using a coupled reaction with oxaloacetate, acetyl-CoA, and 5,5-dithiobis-(2,4-nitrobenzoic acid). Complex I and IV activities were adjusted for total CS in that given fraction (SS or IMF).

Muscle Total RNA and Small RNA Enrichment

Total RNA was isolated from ~25mg of snap frozen muscle tissue using the mirVana™ Paris Kit (Thermo Fisher Scientific, Carlsbad, CA, catalog # AM1556), treated with DNase and checked for genomic DNA contamination by qPCR for GAPDH. RNA was quantified by Small RNA Agilent analysis and reverse transcribed to cDNA using adapter-specific Ion RT primers v2 (Life Technologies, Carlsbad, CA), and enriched for small RNA using two rounds of size selection ethanol washes.

Serum Exosome Isolation and miR Extraction

Exosomes were isolated from 1 mL of serum thawed to room temperature using the Total Exosome Isolation (from serum) kit (Life Technologies), followed by exosomal RNA isolation using the Total Exosome RNA and Protein Isolation Kit (Life Technologies, catalog # 4478545). Exosomal RNA was then converted to cDNA directly using adapter-specific Ion RT primers v2 (Life Technologies, Carlsbad, CA) without Agilent quantitation or enrichment for small RNA.

Small RNA Sequencing

cDNA samples (from both muscle and exosomes) were barcoded using Platinum PCR SuperMix High Fidelity polymerase with IonXpress RNA 3' Barcode primer and unique 5' Ion Xpress RNA-Seq Barcode Primers using the Ion Xpress RNA-Seq Barcode 1-16 Kit (Life Technologies, Carlsbad, CA). The yield and size distribution of the cDNA libraries were assessed using the Agilent 2100 Bioanalyzer DNA1000 chip (Agilent Technologies, Santa Clara, CA). Total barcoded cDNA within the 50 – 300 base pair range was considered to be derived from small RNA. 7.5 picomoles each of 8-10 barcoded libraries were pooled and clonally amplified onto Ion Sphere™ Particles (ISPs) according to the manufacturer's protocol (Ion PI Template OneTouch™ 200 Template Kit v3) and enriched using the Ion OneTouch 2 ES system (Life Technologies, Carlsbad, CA). Small RNA-Seq was performed using the Ion-Torrent platform to identify microRNAs from peripheral which are differentially expressed in serum exosomes and skeletal muscle in response to exercise. Enriched ISPs were sequenced on the Ion Proton Next Generation Sequencing system using the Ion P1 chip v2 Kit and Ion PI™ Sequencing 200 kit v3 (Life Technologies, Carlsbad, CA) with 500 sequencing flows.

miR Differential Expression Analyses

RNA-Seq data processing was performed using Partek Flow v10.0.21.0706 (Partek Inc., Chesterfield, MO). Samples with total read counts less than 200,000 were re-sequenced and the resulting FASTQ files were merged in Partek Flow. Data analysis was performed as described in Sakaram et. al.[94] Briefly, unaligned reads were trimmed to a fixed length based on an average PHRED quality score greater than 20, aligned to miRBase mature miRs version 21 of the hg38 (GRCh38) assembly using a Bowtie aligner, and quantitated using the miRBase version 21 reference. Raw read counts were normalized using the Trimmed Mean of M values (TMM) normalization method with an offset of 1.0 to enable downstream differential expression analysis. TMM normalized read counts and associated raw FASTQ files are available at GSE269533.

Differential Gene Expression (DGE) Analysis

Differential gene expression analysis was performed to identify exercise signatures of the exercise and detraining responses in the full unsegmented dataset and after segmentation on sex (*i.e.,* male and

female), exercise cohort (*i.e.*, TRAD and HITT) and by individual response (i.e. fMQ+/CRF+ vs all non-fMQ+/CRF+. MiR showing differential expression in the untrained (W0) and trained (W12) states were identified by comparing the 3hr "acute" and 24hr timepoints to the corresponding "pre" baseline sample. Training-specific effects were identified by comparing the baseline trained (W12 pre) samples to untrained baseline (W0 pre) samples. Detraining effects were identified by comparing the detrained W16 samples to the trained W12 pre baseline samples. Fold changes and unadjusted p-values were determined using the Lognormal with Shrinkage (LNS) model for Gene Specific Analysis (GSA) in Partek Flow software, v10.0. (2020). Significant differences in miR levels were defined as absolute fold-changes ≥ 1.5, $p \leq 0.05$ and average read count values ≥ 10 in the categories being compared. Detailed fold-change, p-value and average read count information for all DE miR is provided in **Table S1**. UpSet plots were generated in GraphPad Prism version 10.2.1 for Windows (GraphPad Software, Boston, Massachusetts USA, www.graphpad.com).

MiR Target Analysis

mRNA targets of microRNAs showing differential expression were identified using MirTarbase Release 9.0.[95] mRNA targets with weak mean-target interaction (MTI) evidence were removed leaving only those with western blot, reporter assay or qPCR support. Signaling networks were generated using Cytoscape v3.10.2.[96] Core signaling networks were generated by filtering to include only mRNA targeted by 2 or more miR in the dataset.

Pathways Analysis

Pathways analyses of mRNA targets were performed using the KEGG 2021 database via ENRICHR[97] in R with a particular focus on exercise-related pathways and excluding chronic and infectious disease pathways.

QUANTIFICATION AND STATISTICAL ANALYSIS

Data Management

Physical and biological phenotyping data were processed and analyzed using our four-phase data management pipeline (**Figure S5**). All manual entry data fields were double data entered and compared

for discrepancies to ensure accuracy. Where possible, manual data entry was avoided by exporting data from the testing equipment and using parsers built in our data pipeline to process and store the data. All data were processed and organized using R (details provided in Key Resources Table). Quality analysis was performed on test metadata and results, with final data for each participant stored and used for downstream analysis. Values were flagged as outliers and removed when they were above or below 3.6 standard deviations from the mean within each level of the fixed factors (time point). In addition to this we created a model for each variable of interest using W0, W12 and W16 (where applicable) values and then calculated robust mahalanobis distances for each participant from the center of the model for that variable. The model center was determined using minimum covariance determinant which is a more robust method to determine the center of a model when outliers may be present. We then calculated p-values for the mahalanobis distances from a chi-square distribution and potential outliers were flagged for review when $p < 0.001$.

Statistical analyses

Principal outcomes for this per protocol trial were assessed using repeated measures ANOVAs with time (12 weeks of intervention) as the repeated measures factor and intervention (HITT vs. TRAD) as the between groups factor. An *a priori* alpha level of 0.05 was used to determine the main effects of intervention group and time, and group x time interaction. Assumptions of normality, homogeneity of variance and sphericity were assessed statistically and graphically. The assumption of normality of residuals was assessed statistically using Shapiro-Wilks (W: Wilk's Statistic) and Kolmogorov Smirnov tests. Residuals were visualized using QQ and residual plots. Normality of residuals assumption was determined to be violated when 75% or more of the levels of the data were statistically significant. Data that violated the assumption of normality were square root transformed, and normality was re-tested. Homogeneity of variance between groups was assessed using a Levene's test and equality of variance across time was assessed using Maulchy's test of sphericity. If sphericity was violated a Greenhouse-Geisser correction was used to adjust the degrees of freedom for determining the critical value for F to account for the increase in Type I error rate. For targeted muscle tissue analyses where data were

collected at three timepoints (pre-training W0, post-training W12, detraining W16), we used mixed effects models. Variance was estimated using Restricted Maximum Likelihood (REML) and group and time were fixed effects. Intercept was allowed to vary across individual participants (random effect). We calculated degrees of freedom using the Satterwaite method to determine F and p values to test for differences between fixed factors. Significance for all tests was accepted at $p < 0.05$. Where significant interactions or main effects were found, we conducted post-hoc pairwise t-tests on planned comparisons. Where a significant main effect of time existed, we compared W0 vs. W12 and W12 vs. W16. Where significant group by time interactions were detected, we conducted between groups comparisons at W0, W12, W16 and then within groups comparisons (W0 vs. W12, W12 vs. W16) and reported unadjusted p values.

Minimum Clinically Important Difference (MCID) Determination

Thresholds for minimally clinically important difference (MCID) scores were calculated using a distribution-based method for functional muscle quality (fMQ; one repetition maximum of bilateral knee extension normalized to bilateral thigh lean mass) and cardiorespiratory fitness (CRF; VO_{2peak} in L/min). The MCID was determined by multiplying the standard deviation of the individual percent change scores by 0.5 according to established methods.[32] Individuals at or above the MCID threshold for either metric were classified as responders (+) for fMQ and/or CRF. We then created a binary classification as dual responders (fMQ+/CRF+) or non-dual responders (fMQ+/CRF- or fMQ-/CRF+ or fMQ-/CRF-). All responder analyses (differential gene expression (DGE) analysis and HOSVD) were conducted on this binary dual responder outcome (fMQ+/CRF+ vs. all others).

Higher-Order Singular Value Decomposition (HOSVD)

To evaluate potentially important features that may contribute to MCID status, we utilized Tucker decomposition (also known as Higher Order Singular Value Decomposition: HOSVD)[98] to break down high-dimensional data into interpretable components called latent variables (LVs). Phenotypic as well as miR data (muscle miR and serum exosome miR) were used as input features to HOSVD as summarized in **Figure S4**. Phenotyping data were included from W0 and W12. Phenomic variables that had > 20% missing values were removed from the data set and excluded from HOSVD. Where data were retained,

missing values were imputed using the field standard MICE method (Multiple Imputation by Chained Equations).[99] The number of imputations was set to 5 (m=5) and max iterations set to 10. Lasso regression was used primarily, but stochastic regression was also used when appropriate. This resulted in 5 sets of estimated values for each value that was missing; from there we imputed the average estimated value (specific value for a variable for a given participant and time point) for that observation. Baseline miRs at W0 and W12 were included in the model as their raw value whereas miRs at 0h, 3h and 24h were normalized to the baseline (change scores) for that given time point (W0 or W12) and included as the change from baseline in the HOSVD model. HOSVD decomposed the high dimensional data into three key LV matrices: time, participant, and feature LVs. We downselected the 10 feature LVs in which the fMQ+/CRF+ vs. all others MCID classification ranked highest. We then reduced dimensionality in two steps: 1) combined the top 5% of features from each of these top 10 LVs and eliminated any redundancies; and 2) statistically tested each feature between fMQ+/CRF+ and all others using t-tests for continuous data and Chi-Square tests for categorical input features. Welch's t-tests were used when there was unequal variance; otherwise, an equal variance t-test was used. DiVenn networks were generated in DiVenn 1.2.[100]. Canonical pathways impacted were identified using ENRICHR analysis in R as detailed in "Pathway Analysis" above using the Kyoto Encyclopedia of Genes and Genomes (KEGG 2021) pathway database.[97,101] The canonical pathway analysis was conducted on the down-selected miRs that have strong evidence in MirTarbase Release 9.0[95], matching the approach taken in our DGE analysis.

ADDITONAL RESOURCES

The overall trial design is summarized at ClinicalTrials.gov under the protocol identifier NCT03380923 and is available at https://clinicaltrials.gov/study/NCT03380923?id=NCT03380923%20&rank=1.

REFERENCES

1. Piercy KL, Troiano RP, Ballard RM, et al. The Physical Activity Guidelines for Americans. *JAMA*. 2018;320(19):2020-2028. doi:10.1001/jama.2018.14854

2. Harpham C, Gunn H, Marsden J, Connolly L. The feasibility, safety, physiological and clinical effects of high-intensity interval training for people with Parkinson's: a systematic review and meta-analysis. *Aging Clin Exp Res*. 2023;35(3):497-523. doi:10.1007/s40520-022-02330-6

3. Li L, Liu X, Shen F, et al. Effects of high-intensity interval training versus moderate-intensity continuous training on blood pressure in patients with hypertension: A meta-analysis. *Medicine*. 2022;101(50):e32246. doi:10.1097/MD.0000000000032246

4. Casaña J, Varangot-Reille C, Calatayud J, et al. High-Intensity Interval Training (HIIT) on Biological and Body Composition Variables in Patients with Musculoskeletal Disorders: A Systematic Review and Meta-Analysis. *JCM*. 2022;11(23):6937. doi:10.3390/jcm11236937

5. Schulté B, Nieborak L, Leclercq F, Villafañe JH, Sánchez Romero EA, Corbellini C. The Comparison of High-Intensity Interval Training Versus Moderate-Intensity Continuous Training after Coronary Artery Bypass Graft: A Systematic Review of Recent Studies. *JCDD*. 2022;9(10):328. doi:10.3390/jcdd9100328

6. Sabag A, Barr L, Armour M, et al. The Effect of High-intensity Interval Training vs Moderate-intensity Continuous Training on Liver Fat: A Systematic Review and Meta-Analysis. *The Journal of Clinical Endocrinology & Metabolism*. 2022;107(3):862-881. doi:10.1210/clinem/dgab795

7. Wu Q, Niu X, Zhang Y, Song J, Chi A. A Comparative Study of Inhibition Function between High-Intensity Interval Training and Moderate-Intensity Continuous Training in Healthy People: A Systematic Review with Meta-Analysis. *IJERPH*. 2023;20(4):2859. doi:10.3390/ijerph20042859

8. Hu M, Kong Z, Shi Q, Nie J. Acute effect of high-intensity interval training versus moderate-intensity continuous training on appetite-regulating gut hormones in healthy adults: A systematic review and meta-analysis. *Heliyon*. 2023;9(2):e13129. doi:10.1016/j.heliyon.2023.e13129

9. Tamayo Acosta J, Sosa Gomez AE, Samuel S, Pelenyi S, Acosta RE, Acosta M. Effects of Aerobic Exercise Versus High-Intensity Interval Training on V̇O2max and Blood Pressure. *Cureus*. Published online October 15, 2022. doi:10.7759/cureus.30322

10. Keating SE, Johnson NA, Mielke GI, Coombes JS. A systematic review and meta-analysis of interval training versus moderate-intensity continuous training on body adiposity. *Obesity Reviews*. 2017;18(8):943-964. doi:10.1111/obr.12536

11. Lavin KM, Graham ZA, McAdam JS, et al. Dynamic transcriptomic responses to divergent acute exercise stimuli in young adults. *Physiol Genomics*. 2023;55(4):194-212. doi:10.1152/physiolgenomics.00144.2022

12. Sieland J, Niederer D, Engeroff T, et al. Effects of single bouts of different endurance exercises with different intensities on microRNA biomarkers with and without blood flow restriction: a three-arm, randomized crossover trial. *Eur J Appl Physiol*. 2021;121(11):3243-3255. doi:10.1007/s00421-021-04786-2

13. Vogel J, Niederer D, Engeroff T, et al. Effects on the Profile of Circulating miRNAs after Single Bouts of Resistance Training with and without Blood Flow Restriction-A Three-Arm, Randomized Crossover Trial. *Int J Mol Sci*. 2019;20(13):3249. doi:10.3390/ijms20133249

14. Garai K, Adam Z, Herczeg R, et al. Physical Activity as a Preventive Lifestyle Intervention Acts Through Specific Exosomal miRNA Species—Evidence From Human Short- and Long-Term Pilot Studies. *Front Physiol*. 2021;12:658218. doi:10.3389/fphys.2021.658218

15. de Gonzalo-Calvo D, Dávalos A, Montero A, et al. Circulating inflammatory miRNA signature in response to different doses of aerobic exercise. *J Appl Physiol (1985)*. 2015;119(2):124-134. doi:10.1152/japplphysiol.00077.2015

16. Lai Z, Lin W, Yan X, Chen X, Xu G. Fatiguing freestyle swimming modifies miRNA profiles of circulating extracellular vesicles in athletes. *Eur J Appl Physiol*. 2023;123(9):2041-2051. doi:10.1007/s00421-023-05167-7

17. Boehler JF, Hogarth MW, Barberio MD, et al. Effect of endurance exercise on microRNAs in myositis skeletal muscle-A randomized controlled study. *PLoS One*. 2017;12(8):e0183292. doi:10.1371/journal.pone.0183292

18. Ogasawara R, Akimoto T, Umeno T, Sawada S, Hamaoka T, Fujita S. MicroRNA expression profiling in skeletal muscle reveals different regulatory patterns in high and low responders to resistance training. *Physiol Genomics*. 2016;48(4):320-324. doi:10.1152/physiolgenomics.00124.2015

19. Sieland J, Niederer D, Engeroff T, et al. Changes in miRNA expression in patients with peripheral arterial vascular disease during moderate- and vigorous-intensity physical activity. *Eur J Appl Physiol*. 2023;123(3):645-654. doi:10.1007/s00421-022-05091-2

20. Widmann M, Mattioni Maturana F, Burgstahler C, et al. miRNAs as markers for the development of individualized training regimens: A pilot study. *Physiol Rep*. 2022;10(5):e15217. doi:10.14814/phy2.15217

21. Liu HW, Cheng HC, Tsai SH, Sun WH. Effect of Progressive Resistance Training on Circulating Adipogenesis-, Myogenesis-, and Inflammation-Related microRNAs in Healthy Older Adults: An Exploratory Study. *Gerontology*. 2020;66(6):562-570. doi:10.1159/000510148

22. de Gonzalo-Calvo D, Dávalos A, Fernández-Sanjurjo M, et al. Circulating microRNAs as emerging cardiac biomarkers responsive to acute exercise. *Int J Cardiol*. 2018;264:130-136. doi:10.1016/j.ijcard.2018.02.092

23. Margolis LM, Hatch-McChesney A, Allen JT, et al. Circulating and skeletal muscle microRNA profiles are more sensitive to sustained aerobic exercise than energy balance in males. *The Journal of Physiology*. 2022;600(17):3951-3963. doi:10.1113/JP283209

24. Nielsen S, Scheele C, Yfanti C, et al. Muscle specific microRNAs are regulated by endurance exercise in human skeletal muscle. *J Physiol*. 2010;588(Pt 20):4029-4037. doi:10.1113/jphysiol.2010.189860

25. Morgan CP, Bale TL. Sex differences in microRNA regulation of gene expression: no smoke, just miRs. *Biol Sex Differ*. 2012;3(1):22. doi:10.1186/2042-6410-3-22

26. Pak TR, Rao YS, Prins SA, Mott NN. An emerging role for microRNAs in sexually dimorphic neurobiological systems. *Pflugers Arch*. 2013;465(5):655-667. doi:10.1007/s00424-013-1227-y

27. Dai R, Ahmed SA. Sexual dimorphism of miRNA expression: a new perspective in understanding the sex bias of autoimmune diseases. *Ther Clin Risk Manag*. 2014;10:151-163. doi:10.2147/TCRM.S33517

28. Cui C, Cui Q. The relationship of human tissue microRNAs with those from body fluids. *Sci Rep*. 2020;10(1):5644. doi:10.1038/s41598-020-62534-6

29. Margolis LM, Lessard SJ, Ezzyat Y, Fielding RA, Rivas DA. Circulating MicroRNA Are Predictive of Aging and Acute Adaptive Response to Resistance Exercise in Men. *J Gerontol A Biol Sci Med Sci*. 2017;72(10):1319-1326. doi:10.1093/gerona/glw243

30. Erickson ML, Allen JM, Beavers DP, et al. Understanding heterogeneity of responses to, and optimizing clinical efficacy of, exercise training in older adults: NIH NIA Workshop summary. *Geroscience*. 2023;45(1):569-589. doi:10.1007/s11357-022-00668-3

31. Noone J, Mucinski JM, DeLany JP, Sparks LM, Goodpaster BH. Understanding the variation in exercise responses to guide personalized physical activity prescriptions. *Cell Metabolism*. Published online January 2024:S155041312300476X. doi:10.1016/j.cmet.2023.12.025

32. Franceschini M, Boffa A, Pignotti E, Andriolo L, Zaffagnini S, Filardo G. The Minimal Clinically Important Difference Changes Greatly Based on the Different Calculation Methods. *Am J Sports Med*. 2023;51(4):1067-1073. doi:10.1177/03635465231152484

33. Menshikova EV, Ritov VB, Fairfull L, Ferrell RE, Kelley DE, Goodpaster BH. Effects of Exercise on Mitochondrial Content and Function in Aging Human Skeletal Muscle. *The Journals of Gerontology Series A: Biological Sciences and Medical Sciences*. 2006;61(6):534-540. doi:10.1093/gerona/61.6.534

34. Coyle EF, Martin WH, Sinacore DR, Joyner MJ, Hagberg JM, Holloszy JO. Time course of loss of adaptations after stopping prolonged intense endurance training. *J Appl Physiol Respir Environ Exerc Physiol*. 1984;57(6):1857-1864. doi:10.1152/jappl.1984.57.6.1857

35. Coyle EF, Martin WH, Bloomfield SA, Lowry OH, Holloszy JO. Effects of detraining on responses to submaximal exercise. *J Appl Physiol (1985)*. 1985;59(3):853-859. doi:10.1152/jappl.1985.59.3.853

36. Klausen K, Andersen LB, Pelle I. Adaptive changes in work capacity, skeletal muscle capillarization and enzyme levels during training and detraining. *Acta Physiologica Scandinavica*. 1981;113(1):9-16. doi:10.1111/j.1748-1716.1981.tb06854.x

37. Kadi F, Schjerling P, Andersen LL, et al. The effects of heavy resistance training and detraining on satellite cells in human skeletal muscles. *J Physiol*. 2004;558(Pt 3):1005-1012. doi:10.1113/jphysiol.2004.065904

38. Blocquiaux S, Gorski T, Van Roie E, et al. The effect of resistance training, detraining and retraining on muscle strength and power, myofibre size, satellite cells and myonuclei in older men. *Experimental Gerontology*. 2020;133:110860. doi:10.1016/j.exger.2020.110860

39. Murach KA, Mobley CB, Zdunek CJ, et al. Muscle memory: myonuclear accretion, maintenance,

morphology, and miRNA levels with training and detraining in adult mice. *J cachexia sarcopenia muscle*. 2020;11(6):1705-1722. doi:10.1002/jcsm.12617

40. Harber MP, Konopka AR, Undem MK, et al. Aerobic exercise training induces skeletal muscle hypertrophy and age-dependent adaptations in myofiber function in young and older men. *J Appl Physiol (1985)*. 2012;113(9):1495-1504. doi:10.1152/japplphysiol.00786.2012

41. Sale DG, MacDougall JD, Jacobs I, Garner S. Interaction between concurrent strength and endurance training. *J Appl Physiol (1985)*. 1990;68(1):260-270. doi:10.1152/jappl.1990.68.1.260

42. Shamim B, Camera DM, Whitfield J. Myofibre Hypertrophy in the Absence of Changes to Satellite Cell Content Following Concurrent Exercise Training in Young Healthy Men. *Front Physiol*. 2021;12:625044. doi:10.3389/fphys.2021.625044

43. Murach KA, Bagley JR. Skeletal Muscle Hypertrophy with Concurrent Exercise Training: Contrary Evidence for an Interference Effect. *Sports Med*. 2016;46(8):1029-1039. doi:10.1007/s40279-016-0496-y

44. Houmard JA, Hortobágyi T, Johns RA, et al. Effect of Short-Term Training Cessation on Performance Measures in Distance Runners. *Int J Sports Med*. 1992;13(8):572-576. doi:10.1055/s-2007-1024567

45. Houston ME, Bentzen H, Larsen H. Interrelationships between skeletal muscle adaptations and performance as studied by detraining and retraining. *Acta Physiol Scand*. 1979;105(2):163-170. doi:10.1111/j.1748-1716.1979.tb06328.x

46. Glass DJ. PI3 kinase regulation of skeletal muscle hypertrophy and atrophy. *Curr Top Microbiol Immunol*. 2010;346:267-278. doi:10.1007/82_2010_78

47. Brahmer A, Neuberger E, Esch-Heisser L, et al. Platelets, endothelial cells and leukocytes contribute to the exercise-triggered release of extracellular vesicles into the circulation. *J of Extracellular Vesicle*. 2019;8(1):1615820. doi:10.1080/20013078.2019.1615820

48. D'Souza RF, Woodhead JST, Zeng N, et al. Circulatory exosomal miRNA following intense exercise is unrelated to muscle and plasma miRNA abundances. *American Journal of Physiology-Endocrinology and Metabolism*. 2018;315(4):E723-E733. doi:10.1152/ajpendo.00138.2018

49. Silver JL, Alexander SE, Dillon HT, Lamon S, Wadley GD. Extracellular vesicular miRNA expression is not a proxy for skeletal muscle miRNA expression in males and females following acute, moderate intensity exercise. *Physiol Rep*. 2020;8(16). doi:10.14814/phy2.14520

50. Ansdell P, Thomas K, Hicks KM, Hunter SK, Howatson G, Goodall S. Physiological sex differences affect the integrative response to exercise: acute and chronic implications. *Experimental Physiology*. 2020;105(12):2007-2021. doi:10.1113/EP088548

51. Torres-Aguilera I, Pinto-Hernandez P, Iglesias-Gutierrez E, Terrados N, Fernandez-Sanjurjo M. Circulating plasma levels of miR-106b-5p predicts maximal performance in female and male elite kayakers. *Front Sports Act Living*. 2023;5:1040955. doi:10.3389/fspor.2023.1040955

52. Frühbeis C, Helmig S, Tug S, Simon P, Krämer-Albers E. Physical exercise induces rapid release of small extracellular vesicles into the circulation. *J of Extracellular Vesicle*. 2015;4(1):28239.

doi:10.3402/jev.v4.28239

53. Telles GD, Libardi CA, Conceição MS, et al. Time Course of Skeletal Muscle miRNA Expression after Resistance, High-Intensity Interval, and Concurrent Exercise. *Medicine & Science in Sports & Exercise*. 2021;53(8):1708-1718. doi:10.1249/MSS.0000000000002632

54. Cui S, Sun B, Yin X, et al. Time-course responses of circulating microRNAs to three resistance training protocols in healthy young men. *Sci Rep*. 2017;7(1):2203. doi:10.1038/s41598-017-02294-y

55. D'Souza RF, Markworth JF, Aasen KMM, Zeng N, Cameron-Smith D, Mitchell CJ. Acute resistance exercise modulates microRNA expression profiles: Combined tissue and circulatory targeted analyses. Lamon S, ed. *PLoS ONE*. 2017;12(7):e0181594. doi:10.1371/journal.pone.0181594

56. Buchanan SR, Miller RM, Nguyen M, et al. Circulating microRNA responses to acute whole-body vibration and resistance exercise in postmenopausal women. *Front Endocrinol*. 2022;13:1038371. doi:10.3389/fendo.2022.1038371

57. Mosteiro L, Pantoja C, de Martino A, Serrano M. Senescence promotes in vivo reprogramming through p16INK4a and IL-6. *Aging Cell*. 2018;17(2):e12711. doi:10.1111/acel.12711

58. Wang MJ, Zhang HL, Chen F, Guo XJ, Liu QG, Hou J. The double-edged effects of IL-6 in liver regeneration, aging, inflammation, and diseases. *Experimental Hematology & Oncology*. 2024;13(1):62. doi:10.1186/s40164-024-00527-1

59. Luo Z, Yao J, Wang Z, Xu J. Mitochondria in endothelial cells angiogenesis and function: current understanding and future perspectives. *Journal of Translational Medicine*. 2023;21(1):441. doi:10.1186/s12967-023-04286-1

60. Sun F, Bi Q, Wang X, Liu J. Down-regulation of mir-27b promotes angiogenesis and fibroblast activation through activating PI3K/AKT signaling pathway. *Wound Repair Regen*. 2020;28(1):39-48. doi:10.1111/wrr.12765

61. Ke Q, Costa M. Hypoxia-inducible factor-1 (HIF-1). *Mol Pharmacol*. 2006;70(5):1469-1480. doi:10.1124/mol.106.027029

62. Ioannilli L, Ciccarone F, Ciriolo MR. Adipose Tissue and FoxO1: Bridging Physiology and Mechanisms. *Cells*. 2020;9(4):849. doi:10.3390/cells9040849

63. Li F, Bai M, Xu J, Zhu L, Liu C, Duan R. Long-Term Exercise Alters the Profiles of Circulating Micro-RNAs in the Plasma of Young Women. *Front Physiol*. 2020;11:372. doi:10.3389/fphys.2020.00372

64. Haoran S, Zhishan J, Yan M, et al. Hypoxic Preconditioning Enhances Cellular Viability and Migratory Ability: Role of DANCR/miR-656-3p/HIF-1α Axis in Placental Mesenchymal Stem Cells. *Stem Cells*. 2023;41(9):877-891. doi:10.1093/stmcls/sxad048

65. Amani M, Rahmati M, Fathi M, Ahmadvand H. Reduce Muscle Fibrosis through Exercise via NRG1/ErbB2 Modification in Diabetic Rats. *J Diabetes Res*. 2020;2020:6053161. doi:10.1155/2020/6053161

66. Jiewei Y, Jingjing Z, Jingjing X, Guilan Z. Downregulation of circ-UBAP2 ameliorates oxidative stress

and dysfunctions of human retinal microvascular endothelial cells (hRMECs) via miR-589-5p/EGR1 axis. *Bioengineered*. 2021;12(1):7508-7518. doi:10.1080/21655979.2021.1979440

67. Semenova EA, Zempo H, Miyamoto-Mikami E, et al. Genome-Wide Association Study Identifies CDKN1A as a Novel Locus Associated with Muscle Fiber Composition. *Cells*. 2022;11(23):3910. doi:10.3390/cells11233910

68. Davey EE, Légaré C, Planco L, et al. Individual transcriptomic response to strength training for patients with myotonic dystrophy type 1. *JCI Insight*. 2023;8(14):e163856. doi:10.1172/jci.insight.163856

69. Aguilar S, García-Olloqui P, Amigo-Morán L, et al. Cardiac Progenitor Cell Exosomal miR-935 Protects against Oxidative Stress. *Cells*. 2023;12(18):2300. doi:10.3390/cells12182300

70. You J, Sun L, Wang J, et al. Role of Adiponectin-Notch pathway in cognitive dysfunction associated with depression and in the therapeutic effect of physical exercise. *Aging Cell*. 2021;20(6):e13387. doi:10.1111/acel.13387

71. Gavin TP, Drew JL, Kubik CJ, Pofahl WE, Hickner RC. Acute resistance exercise increases skeletal muscle angiogenic growth factor expression. *Acta Physiol (Oxf)*. 2007;191(2):139-146. doi:10.1111/j.1748-1716.2007.01723.x

72. Mei T, Hu Y, Zhang Y, Li Y. Hypoxia treatment and resistance training alters microRNA profiling in rats skeletal muscle. *Sci Rep*. 2024;14(1):8388. doi:10.1038/s41598-024-58996-7

73. Zhang Y, Yao Y, Wei J, Zhang Z. miR-338-5p regulated the NF-κB/MAPK pathway to alleviate inflammation and oxidative stress by targeting IL-6 in rats with atrial fibrillation. *3 Biotech*. 2024;14(7):182. doi:10.1007/s13205-024-04024-4

74. Zhang T, Brinkley TE, Liu K, et al. Circulating MiRNAs as biomarkers of gait speed responses to aerobic exercise training in obese older adults. *Aging (Albany NY)*. 2017;9(3):900-913. doi:10.18632/aging.101199

75. Zhang B, Tian X, Qu Z, Hao J, Zhang W. Hypoxia-Preconditioned Extracellular Vesicles from Mesenchymal Stem Cells Improve Cartilage Repair in Osteoarthritis. *Membranes (Basel)*. 2022;12(2):225. doi:10.3390/membranes12020225

76. Wang Y, Li F, Gao X, et al. miR-181d-5p ameliorates hypercholesterolemia by targeting PCSK9. *J Endocrinol*. 2024;262(3):e230402. doi:10.1530/JOE-23-0402

77. Zhang Y, Li C, Guan C, et al. MiR-181d-5p Targets KLF6 to Improve Ischemia/Reperfusion-Induced AKI Through Effects on Renal Function, Apoptosis, and Inflammation. *Front Physiol*. 2020;11:510. doi:10.3389/fphys.2020.00510

78. Yang Q, Chen S, Wang X, et al. Exercise Mitigates Endothelial Pyroptosis and Atherosclerosis by Downregulating NEAT1 Through N6-Methyladenosine Modifications. *Arterioscler Thromb Vasc Biol*. 2023;43(6):910-926. doi:10.1161/ATVBAHA.123.319251

79. Zhang M, Wang X, Yao J, Qiu Z. Long non-coding RNA NEAT1 inhibits oxidative stress-induced vascular endothelial cell injury by activating the miR-181d-5p/CDKN3 axis. *Artif Cells Nanomed Biotechnol*. 2019;47(1):3129-3137. doi:10.1080/21691401.2019.1646264

80. Landau W. The targets R package: a dynamic Make-like function-oriented pipeline toolkit for reproducibility and high-performance computing. *JOSS*. 2021;6(57):2959. doi:10.21105/joss.02959

81. Wickham H, Averick M, Bryan J, et al. tidyverse. Published online November 19, 2019. doi:10.5281/ZENODO.3547813

82. Bates D, Mächler M, Bolker B, Walker S. Fitting Linear Mixed-Effects Models Using **lme4**. *J Stat Soft*. 2015;67(1). doi:10.18637/jss.v067.i01

83. Michael A. Lawrence. ez: Easy Analysis and Visualization of Factorial Experiments. Published online 2016. Accessed December 21, 2024. https://CRAN.R-project.org/package=ez

84. Drummer DJ, McAdam JS, Seay R, et al. Perioperative assessment of muscle inflammation susceptibility in patients with end-stage osteoarthritis. *J Appl Physiol (1985)*. 2022;132(4):984-994. doi:10.1152/japplphysiol.00428.2021

85. Roberts BM, Lavin KM, Many GM, et al. Human neuromuscular aging: Sex differences revealed at the myocellular level. *Exp Gerontol*. 2018;106:116-124. doi:10.1016/j.exger.2018.02.023

86. Kelly NA, Hammond KG, Stec MJ, et al. Quantification and characterization of grouped type I myofibers in human aging. *Muscle and Nerve*. 2018;57(1). doi:10.1002/mus.25711

87. Lavin KM, Bell MB, McAdam JS, et al. Muscle transcriptional networks linked to resistance exercise training hypertrophic response heterogeneity. *Physiol Genomics*. 2021;53(5):206-221. doi:10.1152/physiolgenomics.00154.2020

88. Walton RG, Dungan CM, Long DE, et al. Metformin blunts muscle hypertrophy in response to progressive resistance exercise training in older adults: A randomized, double-blind, placebo-controlled, multicenter trial: The MASTERS trial. *Aging Cell*. 2019;18(6):e13039. doi:10.1111/acel.13039

89. Stec MJ, Thalacker-Mercer A, Mayhew DL, et al. Randomized, four-arm, dose-response clinical trial to optimize resistance exercise training for older adults with age-related muscle atrophy. *Exp Gerontol*. 2017;99:98-109. doi:10.1016/j.exger.2017.09.018

90. Kelly NA, Hammond KG, Bickel CS, Windham ST, Tuggle SC, Bamman MM. Effects of aging and Parkinson's disease on motor unit remodeling: influence of resistance exercise training. *J Appl Physiol (1985)*. 2018;124(4):888-898. doi:10.1152/japplphysiol.00563.2017

91. Wen Y, Murach KA, Vechetti IJ, et al. MyoVision: software for automated high-content analysis of skeletal muscle immunohistochemistry. *J Appl Physiol (1985)*. 2018;124(1):40-51. doi:10.1152/japplphysiol.00762.2017

92. Rasmussen HN, Andersen AJ, Rasmussen UF. Optimization of preparation of mitochondria from 25-100 mg skeletal muscle. *Anal Biochem*. 1997;252(1):153-159. doi:10.1006/abio.1997.2304

93. Kelly NA, Ford MP, Standaert DG, et al. Novel, high-intensity exercise prescription improves muscle mass, mitochondrial function, and physical capacity in individuals with Parkinson's disease. *Journal of applied physiology (Bethesda, Md : 1985)*. 2014;116(5):582-592. doi:10.1152/japplphysiol.01277.2013

94. Sakaram S, Craig MP, Hill NT, et al. Identification of novel ΔNp63α-regulated miRNAs using an optimized small RNA-Seq analysis pipeline. *Sci Rep*. 2018;8(1):10069. doi:10.1038/s41598-018-28168-5

95. Huang HY, Lin YCD, Cui S, et al. miRTarBase update 2022: an informative resource for experimentally validated miRNA-target interactions. *Nucleic Acids Res*. 2022;50(D1):D222-D230. doi:10.1093/nar/gkab1079

96. Shannon P, Markiel A, Ozier O, et al. Cytoscape: a software environment for integrated models of biomolecular interaction networks. *Genome Res*. 2003;13(11):2498-2504. doi:10.1101/gr.1239303

97. Chen EY, Tan CM, Kou Y, et al. Enrichr: interactive and collaborative HTML5 gene list enrichment analysis tool. *BMC Bioinformatics*. 2013;14:128. doi:10.1186/1471-2105-14-128

98. Ahmadi-Asl S, Abukhovich S, Asante-Mensah MG, et al. Randomized Algorithms for Computation of Tucker Decomposition and Higher Order SVD (HOSVD). *IEEE Access*. 2021;9:28684-28706. doi:10.1109/ACCESS.2021.3058103

99. Buuren SV, Groothuis-Oudshoorn K. **mice** : Multivariate Imputation by Chained Equations in *R*. *J Stat Soft*. 2011;45(3). doi:10.18637/jss.v045.i03

100. Sun L, Dong S, Ge Y, et al. DiVenn: An Interactive and Integrated Web-Based Visualization Tool for Comparing Gene Lists. *Front Genet*. 2019;10:421. doi:10.3389/fgene.2019.00421

101. Gene Set Knowledge Discovery with Enrichr - Xie - 2021 - Current Protocols - Wiley Online Library. Accessed November 8, 2024. https://currentprotocols.onlinelibrary.wiley.com/doi/10.1002/cpz1.90

Table 1. In vivo physiological and performance phenotyping adaptations to HITT and TRAD exercise training.

Prescription (Rx)	**HITT**		**TRAD**		**Model Results**		
Variable	**Pre-training Mean (SD)**	**Post-training Mean (SD)**	**Pre-training Mean (SD)**	**Post-training Mean (SD)**	**Time (P-value)**	**Rx (P-value)**	**Intrxn (P-value)**
Aerobic Power (cardiorespiratory fitness, CRF)							
VO_2peak (L/min)	2.36 (0.71)	2.62 (0.70)	2.35 (0.63)	2.60 (0.68)	**< 0.001**	0.911	0.948
VO_2peak (mL/kg/min)	33.16 (7.10)	36.58 (7.08)	33.16 (6.77)	36.75 (7.04)	**< 0.001**	0.951	0.862
Peak heart rate (bt/min)	188.6 (9.8)	185.1 (8.4)	191.5 (9.7)	186.1 (10.6)	**< 0.001**	0.376	0.237
Peak RER (VCO_2/VO_2)	1.295 (0.083)	1.253 (0.069)	1.288 (0.078)	1.265 (0.059)	**< 0.001**	0.864	0.227
Peak oxygen pulse (ml O_2/beat)	13.12 (4.94)	14.35 (4.10)	12.40 (3.65)	14.73 (4.44)	**< 0.001**	0.865	0.144
Peak power (W)	181.1 (60.3)	206.0 (58.6)	184.9 (60.4)	212.3 (63.0)	**< 0.001**	0.698	0.629
Anaerobic Power (30-s Wingate)							
Peak power (W)	639.6 (198.8)	771.9 (217.1)	664.4 (252.5)	741.5 (198.4)	**< 0.001**	0.949	0.068
Peak power (W/kg)	8.87 (2.03)	10.60 (2.11)	9.27 (2.61)	10.44 (1.94)	**< 0.001**	0.779	0.181
Rate of fatigue (%)	54.1 (13.9)	61.1 (12.8)	58.1 (18.5)	55.0 (11.5)	0.298	0.661	**0.009**
Neuromuscular Strength and Power							
1RM squat (kg)	71.07 (29.77)	91.50 (29.46)	72.24 (31.50)	89.92 (33.02)	**< 0.001**	0.965	0.765
1RM knee extension (kg)	86.13 (34.91)	107.51 (38.21)	81.33 (28.94)	101.72 (37.78)	**< 0.001**	0.314	0.925
1RM chest press (kg)	51.96 (27.05)	62.64 (27.65)	50.45 (26.28)	57.97 (26.70)	**0.023**	0.441	0.693
1RM overhead press (kg)	36.87 (15.72)	41.46 (16.59)	35.37 (16.48)	40.99 (16.36)	**0.037**	0.685	0.831
1RM lat pulldown (kg)	51.21 (17.56)	59.39 (18.61)	47.44 (20.30)	53.52 (19.71)	**0.012**	0.089	0.711
Unilateral knee extension MVIC (N·m)	196.4 (70.0)	221.4 (75.2)	183.9 (57.4)	210.2 (65.9)	**< 0.001**	0.393	0.842
Unilateral knee extension power (W)	183.0 (96.9)	228.3 (110.7)	157.5 (92.0)	211.0 (97.6)	**< 0.001**	0.278	0.590
Body Composition							
Total lean mass (kg)	46.46 (9.75)	47.69 (9.75)	45.04 (9.93)	46.35 (10.18)	**< 0.001**	0.533	0.796
Bilateral thigh lean mass (g)	11994 (2892)	12330 (2664)	11503 (2749)	11953 (2827)	**< 0.001**	0.465	0.514
Bilateral arm lean mass (g)	5432 (1805)	5658 (1829)	5379 (1896)	5582 (1922)	**< 0.001**	0.874	0.685
Total fat mass (kg)	21.68 (7.31)	20.64 (6.90)	21.18 (7.09)	20.23 (7.36)	**< 0.001**	0.775	0.823
Visceral fat mass (g)	333 (288)	295 (284)	307 (266)	295 (253)	**0.004**	0.823	0.129
Subcutaneous abdominal fat mass (g)	1179 (690)	1102 (667)	1255 (623)	1133 (636)	**< 0.001**	0.704	0.215
Bodyfat percentage (%)	30.44 (8.52)	28.94 (8.14)	30.67 (8.53)	29.18 (8.99)	**< 0.001**	0.902	0.982

Table 2. *Ex vivo* skeletal muscle phenotyping of adaptations to HITT and TRAD exercise training.

Prescription (Rx)	**HITT**			**TRAD**			**Mixed Effects Results**		
Variable (post hoc contrasts noted)	**Pre-training Mean (SD)**	**Post-training Mean (SD)**	**Detraining Mean (SD)**	**Pre-training Mean (SD)**	**Post-training Mean (SD)**	**Detraining Mean (SD)**	**Time (P-value)**	**Rx (P-value)**	**Intrxn (P-value)**
Myofiber Cross-sectional Area (fCSA, μm^2)									
Type I (*†)	3610 (950)	3827 (1116)	3561 (1011)	3258 (793)	3851 (904)	3539 (890)	**< 0.001**	0.477	0.062
Type II	3815 (977)	4263 (1224)*	3653 (1092)†	3471 (937)	4162 (1059)*	3964 (1126)	< 0.001	0.700	**0.018**
Mean	3825 (930)	4111 (1048)	3633 (990)†	3394 (728)	4060 (935)*	3842 (973)	< 0.001	0.567	**0.008**
Myofiber Type Distribution (%)									
Type I	31.8 (7.1)	35.2 (8.1)	36.0 (10.7)	34.0 (6.7)	33.6 (12.0)	31.3 (9.3)	0.108	0.320	0.083
Type IIa	62.2 (8.1)	59.9 (8.9)	59.2 (11.5)	60.5 (6.8)	61.2 (12.2)	63.7 (9.2)	0.546	0.324	0.179
Type IIx/IIax	2.1 (3.1)	1.8 (2.6)	1.8 (3.1)	2.3 (2.9)	2.2 (3.0)	1.5 (2.1)	0.107	0.449	0.562
Type I/IIa	4.0 (3.2)	3.1 (3.3)	3.1 (2.5)	3.2 (2.5)	3.0 (2.5)	3.5 (3.7)	0.575	0.649	0.429
Capillarity									
Caps / Type I myofiber (*)	4.19 (1.18)	4.54 (0.99)	4.66 (1.02)	3.83 (0.74)	4.59 (0.91)	4.50 (0.79)	**< 0.001**	0.352	0.109
Caps / Type II myofiber	4.06 (1.20)	4.46 (0.81)*	4.35 (1.04)	3.49 (0.95)	4.44 (0.91)*	4.45 (1.02)	< 0.001	0.396	**0.018**
Cap density (caps/mm^2)	276.2 (96.7)	284.4 (80.4)	294.8 (89.26)	268.2 (69.4)	276.1 (72.1)	301.1 (81.0)	0.193	0.803	0.842
Pax7$^+$ Satellite Cells (SCs)									
SCs / 100 Type I	2.43 (2.49)	2.35 (1.63)	3.30 (2.96)	3.35 (2.36)	5.00 (5.03)*	2.91 (2.80)†	0.348	0.022	**0.025**
SCs / 100 Type II (*†)	1.19 (0.92)	2.03 (1.46)	1.44 (0.875)	1.92 (1.65)	3.59 (2.89)	1.73 (1.85)	**< 0.001**	**0.002**	0.124
SCs / 100 myofibers	1.69 (1.51)	2.15 (1.32)	1.98 (1.202)	2.24 (1.47)	4.33 (3.68)*	1.99 (1.69)†	< 0.001	0.007	**0.006**
Subsarcolemmal (SS) and Intermyofibrillar (IMF) Mitochondrial Enzyme Activities									
SS CS (mU/mg) (*†)	116.2 (74.0)	153.0 (95.0)	113.2 (76.8)	111.1 (89.0)	127.6 (92.6)	107.1 (77.7)	**0.002**	0.525	0.359
SS cx I (μM/min/mU CS)	0.223 (0.127)	0.202 (0.131)	0.243 (0.150)	0.282 (0.232)	0.348 (0.276)	0.320 (0.259)	0.493	**0.011**	0.203
SS cx IV (k/sec/mU CS)	34.60 (27.59)	36.15 (23.15)	33.53 (22.99)	39.86 (34.92)	49.08 (43.90)	34.48 (21.45)	0.060	0.240	0.265
IMF CS (mU/mg)	61.7 (42.2)	89.0 (54.0)*	63.5 (48.4)†	62.0 (55.8)	69.9 (61.2)	72.9 (65.4)	**0.002**	0.734	**0.024**
IMF cx I (μM/min/mU CS)	0.172 (0.120)	0.190 (0.125)	0.176 (0.126)	0.222 (0.176)	0.228 (0.167)	0.251 (0.188)	0.501	0.066	0.661
IMF cx IV (k/sec/mU CS)	15.10 (10.72)	15.48 (12.16)	15.35 (11.41)	16.81 (12.96)	16.27 (10.81)	17.64 (10.89)	0.827	0.418	0.985
Total CS (mU/mg) (*†)	81.6 (60.5)	100.7 (64.4)	85.7 (61.0)	85.6 (69.3)	101.8 (67.5)	90.7 (74.0)	**< 0.001**	0.798	0.953
Serum Cytokines									
IFN-γ (pg/mL)	5.042 (2.223)	5.667 (2.560)	N/A	6.152 (4.731)	6.882 (5.683)	N/A	0.234	0.089	0.926
IL-10 (pg/mL)	0.361 (0.157)	0.418 (0.224)	N/A	0.377 (0.270)	0.546 (0.908)	N/A	0.132	0.344	0.455
IL-12 p70 (pg/mL)	0.306 (0.203)	0.328 (0.222)	N/A	0.221 (0.102)	0.257 (0.155)	N/A	0.149	0.080	0.726
Il-6 (pg/mL)	0.683 (0.388)	0.658 (0.364)	N/A	0.662 (0.409)	0.663 (0.443)	N/A	0.770	0.922	0.752
Il-8 (pg/mL)	9.734 (3.070)	10.587 (4.079)	N/A	8.570 (2.684)	9.049 (2.456)	N/A	0.066	**0.023**	0.604
TNF-α (pg/mL)	2.644 (0.644)	2.689 (0.662)	N/A	2.557 (0.606)	2.637 (0.680)	N/A	0.194	0.594	0.705

A.

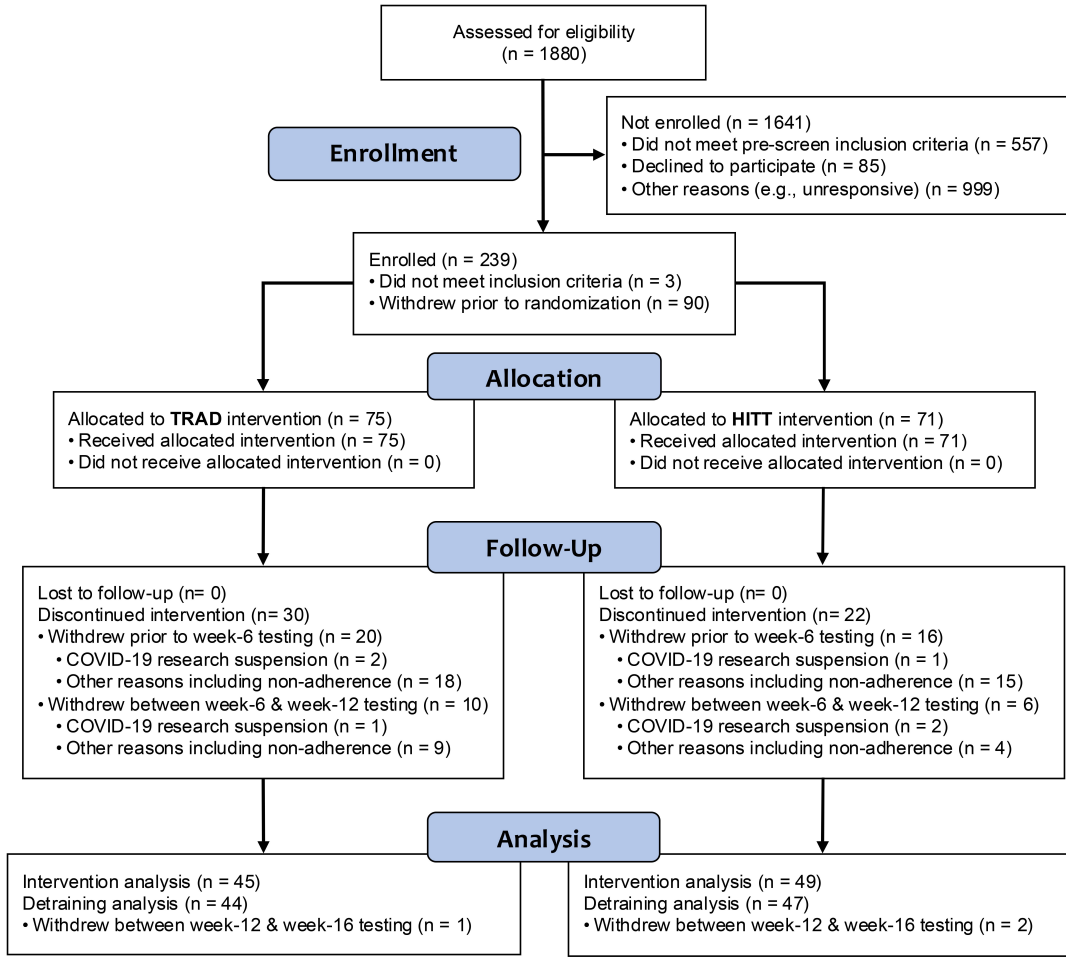

B.

Sex (assigned at birth)	**Females**		**Males**		**All Participants**	**Mixed Effects Results**	
Prescription (Rx)	**HITT (N=28)**	**TRAD (N=22)**	**HITT (N=21)**	**TRAD (N=23)**	**N=94**	**Rx**	**Sex**
Demographics	**Mean (SD)**	**Mean (SD)**	**Mean (SD)**	**Mean (SD)**	**Mean (SD)**	**P-value**	**P-value**
Age (y)	23.3 (2.8)	23.3 (3.0)	23.6 (2.9)	22.8 (3.1)	23.3 (2.9)	0.536	0.831
Height (cm)	165.9 (7.1)	164.0 (7.6)	178.4 (7.7)	177.7 (6.7)	171.0 (9.7)	0.736	**< 0.001**
Weight (kg)	66.0 (10.0)	63.8 (10.6)	78.3 (12.2)	76.6 (10.7)	70.8 (12.4)	0.619	**< 0.001**
IQ Score	116.5 (7.5)	114.8 (10.3)	119.4 (7.3)	121.3 (8.7)	117.6 (8.8)	0.955	**0.020**
Performance IQ Score	114.8 (7.5)	115.6 (12.6)	117.3 (8.1)	118.8 (11.3)	116.4 (10.0)	0.625	0.223
Verbal IQ Score	116.1 (8.2)	112.2 (8.6)	118.3 (8.0)	121.3 (7.8)	116.5 (8.7)	0.618	**0.005**
Race	**N (%)**	**N (%)**	**N (%)**	**N (%)**	**N (%)**		
African American	4 (14.3%)	1 (4.5%)	4 (19.0%)	1 (4.3%)	10 (10.6%)	0.174	0.664
Caucasian	20 (71.4%)	19 (86.4%)	14 (66.7%)	17 (73.9%)	70 (74.5%)		
Other	4 (14.3%)	2 (9.1%)	3 (14.3%)	5 (21.7%)	14 (14.9%)		
Hormone/GF Panel	**Mean (SD)**	**Mean (SD)**	**Mean (SD)**	**Mean (SD)**	**Mean (SD)**		
Testosterone (ng/dL)	46.3 (35.2)	53.4 (28.6)	722.5 (246.9)	670.0 (269.2)	345.6 (367.3)	0.562	**< 0.001**
DHEA (ug/dL)	274.0 (132.3)	300.1 (143.2)	339.0 (112.9)	443.8 (165.0)	336.0 (153.1)	**0.023**	**< 0.001**
SHBG (nmol/L)	75.0 (51.4)	77.3 (38.1)	39.2 (13.8)	34.0 (16.1)	58.0 (40.3)	0.525	**< 0.001**
Androstenedione (ng/mL)	2.69 (1.43)	3.12 (1.45)	2.33 (0.79)	2.23 (0.64)	2.60 (1.20)	0.661	**0.019**
IGF-1 (ng/mL)	288.9 (80.7)	274.2 (59.2)	275.6 (79.6)	276.1 (77.3)	279.5 (74.0)	0.596	0.679
IGFBP-3 (ng/mL)	3565.7 (686.9)	3497.6 (317.0)	3452.1 (485.5)	3434.4 (574.6)	3493.4 (541.0)	0.636	0.422
FGF-21 (pg/mL)	136.7 (119.1)	124.0 (81.9)	111.5 (88.7)	110.3 (55.0)	122.7 (91.6)	0.638	0.359

IQ, intelligence quotient; GF, growth factor; DHEA, dehydroepiandrosterone; SHBG, sex-hormone binding globulin; IGF-I, insulin-like growth factor 1; IGFBP3, IGF binding protein 3; FGF-21, fibroblast growth factor 21

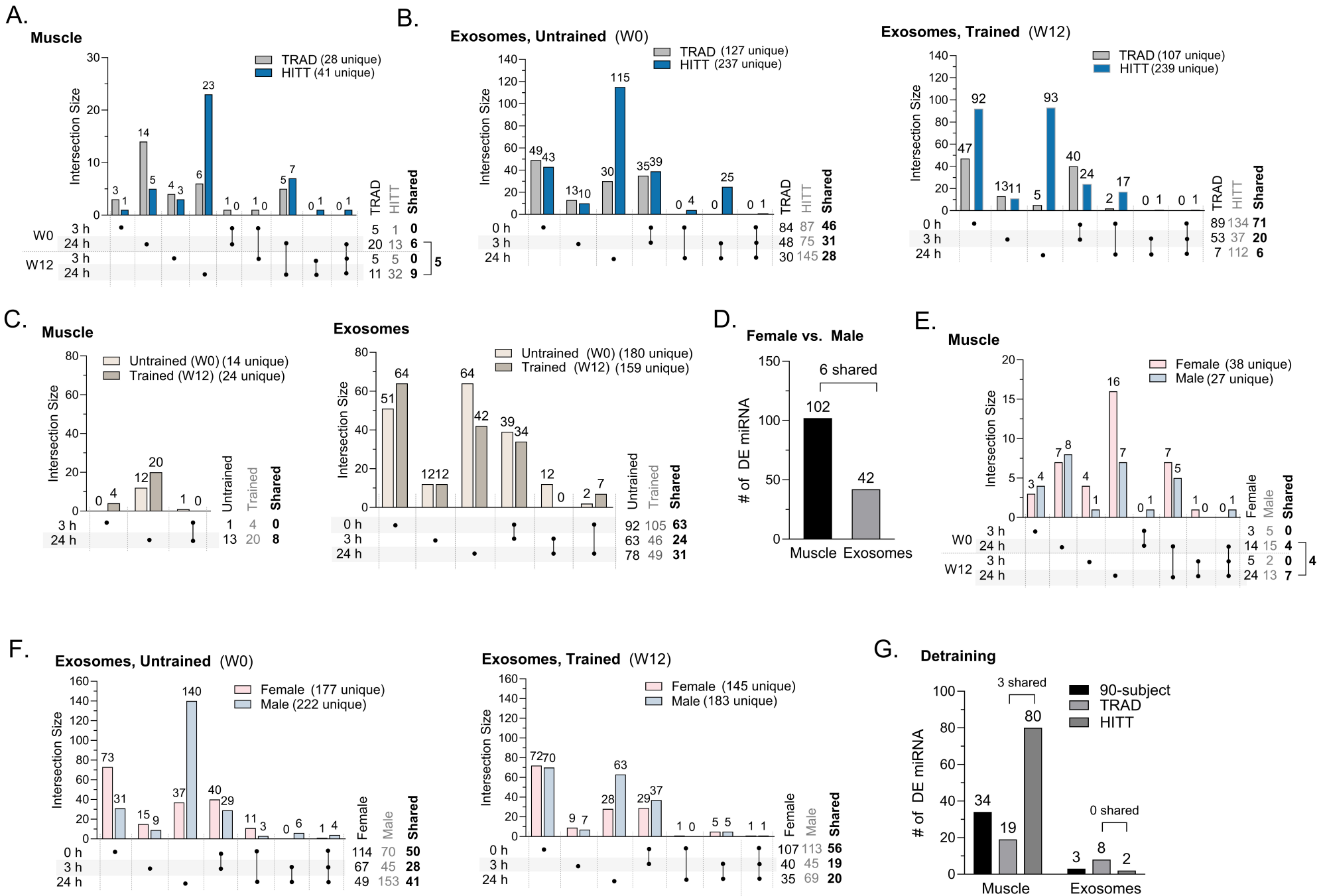
A.
Muscle
TRAD (28 unique)
HITT (41 unique)
Intersection Size
TRAD HITT Shared
W0 3 h 5 1 0
24 h 20 13 6
W12 3 h 5 5 0
24 h 11 32 9
5
B.
Exosomes, Untrained (W0)
TRAD (127 unique)
HITT (237 unique)
Intersection Size
TRAD HITT Shared
0 h 84 87 46
3 h 48 75 31
24 h 30 145 28
Exosomes, Trained (W12)
TRAD (107 unique)
HITT (239 unique)
Intersection Size
TRAD HITT Shared
0 h 89 134 71
3 h 53 37 20
24 h 7 112 6
C.
Muscle
Untrained (W0) (14 unique)
Trained (W12) (24 unique)
Intersection Size
Untrained Trained Shared
3 h 1 4 0
24 h 13 20 8
Exosomes
Untrained (W0) (180 unique)
Trained (W12) (159 unique)
Intersection Size
Untrained Trained Shared
0 h 92 105 63
3 h 63 46 24
24 h 78 49 31
D.
Female vs. Male
6 shared
# of DE miRNA
102
42
Muscle Exosomes
E.
Muscle
Female (38 unique)
Male (27 unique)
Intersection Size
Female Male Shared
W0 3 h 3 5 0
24 h 14 15 4
W12 3 h 5 2 0
24 h 24 13 7
4
F.
Exosomes, Untrained (W0)
Female (177 unique)
Male (222 unique)
Intersection Size
Female Male Shared
0 h 114 70 50
3 h 67 45 28
24 h 49 153 41
Exosomes, Trained (W12)
Female (145 unique)
Male (183 unique)
Intersection Size
Female Male Shared
0 h 107 113 56
3 h 40 45 19
24 h 35 69 20
G.
Detraining
3 shared
90-subject
TRAD
HITT
# of DE miRNA
34
19
80
0 shared
3
8
2
Muscle Exosomes

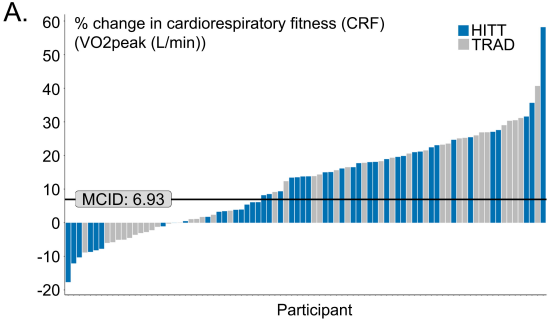
A.
% change in cardiorespiratory fitness (CRF)
(VO2peak (L/min))
HITT
TRAD
MCID: 6.93
Participant

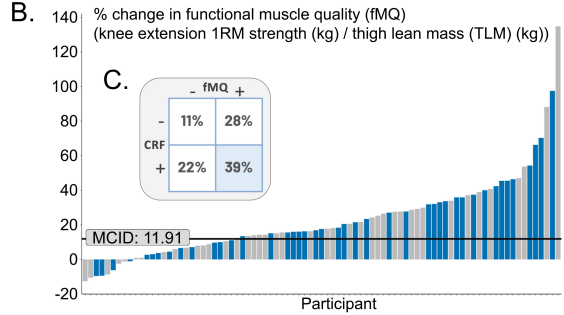
B.
% change in functional muscle quality (fMQ)
(knee extension 1RM strength (kg) / thigh lean mass (TLM) (kg))
C.
fMQ
CRF
11%
28%
22%
39%
MCID: 11.91
Participant

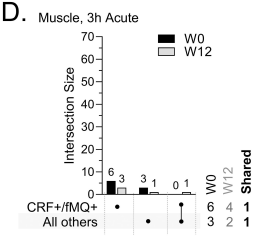
D.
Muscle, 3h Acute
W0
W12
Intersection Size
CRF+/fMQ+
All others
W0 W12 Shared
6 4 1
3 2 1

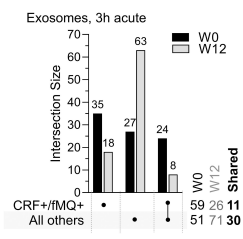
Exosomes, 3h acute
W0
W12
Intersection Size
CRF+/fMQ+
All others
W0 W12 Shared
59 26 11
51 71 30

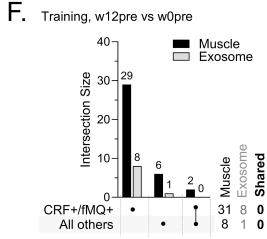
F.
Training, w12pre vs w0pre
Muscle
Exosome
Intersection Size
CRF+/fMQ+
All others
Muscle Exosome Shared
31 8 0
8 1 0

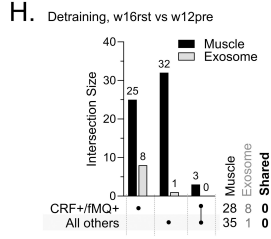
H.
Detraining, w16rst vs w12pre
Muscle
Exosome
Intersection Size
CRF+/fMQ+
All others
Muscle Exosome Shared
28 8 0
35 1 0

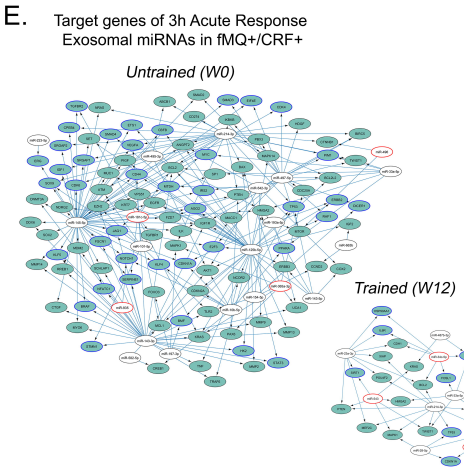
E.
Target genes of 3h Acute Response
Exosomal miRNAs in fMQ+/CRF+
Untrained (W0)
Trained (W12)

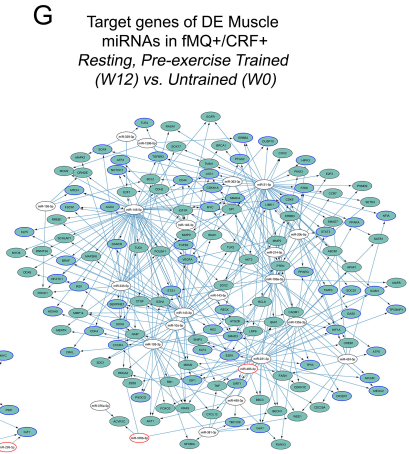
G
Target genes of DE Muscle
miRNAs in fMQ+/CRF+
Resting, Pre-exercise Trained
(W12) vs. Untrained (W0)

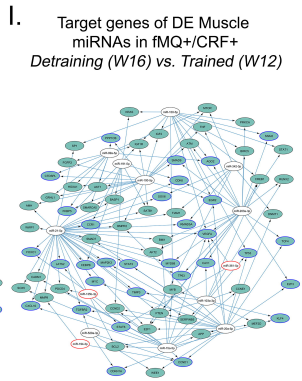
I.
Target genes of DE Muscle
miRNAs in fMQ+/CRF+
Detraining (W16) vs. Trained (W12)

A.

CRF \ fMQ	-	+
-	11% 3F, 6M	28% 14F, 9M
+	22% 10F, 8M	39% 17F, 14M

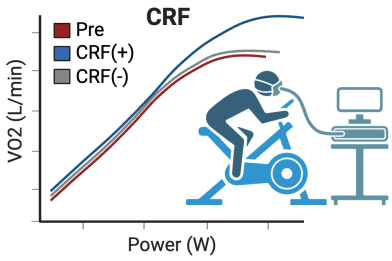

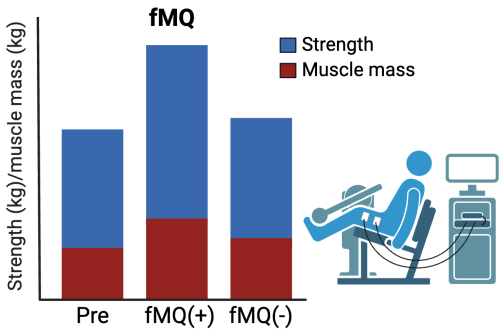

B.

Model inputs (features)

In vivo phenomics
- age, sex, ethnicity, race
- height, weight, BMI
- medical history
- medication history
- health & lifestyle history
- cognitive function
- body composition including total and partitioned:
  - fat mass
  - lean mass
  - bone mineral density
- cardiorespiratory fitness
- anaerobic power
- functional muscle quality
- neuromuscular strength
- neuromuscular power

Muscle tissue ex vivo phenomics
- myofiber type distribution
- myofiber cross-sectional area
- capillary supply
- stem cell distribution
- mitochondrial biogenesis & function

Multiomics & inter-tissue communication
- serum
  - extracellular vesicles miRNA-Seq
  - inflammatory cytokines
  - hormones & growth factors
- skeletal muscle
  - miRNA-Seq

C.

Pre-training differences		Post-training differences	
↓	Workplace physical demands		
↓	Lifestyle physical demands		
↓	Habitual caffeine		
↓	Habitual alcohol		
↓	Android fat mass	↑	Loss of android fat
↓	Android subcutaneous fat	↑	Loss of android subcutaneous fat
↓	Arm fat mass		
↓	Knee extensor fatigability		
↓	Capillary density	↑	Increase in capillary density
↓	Capillaries per type I myofiber	↑	Increase in capillaries per type I myofiber
↓	Serum IL-6		
65	Resting muscle miRs	67	Resting muscle miRs
90	Acute response muscle miRs	90	Acute response muscle miRs
54	Resting EV miRs	36	Resting EV miRs
126	Acute response EV miRs	123	Acute response EV miRs

D.

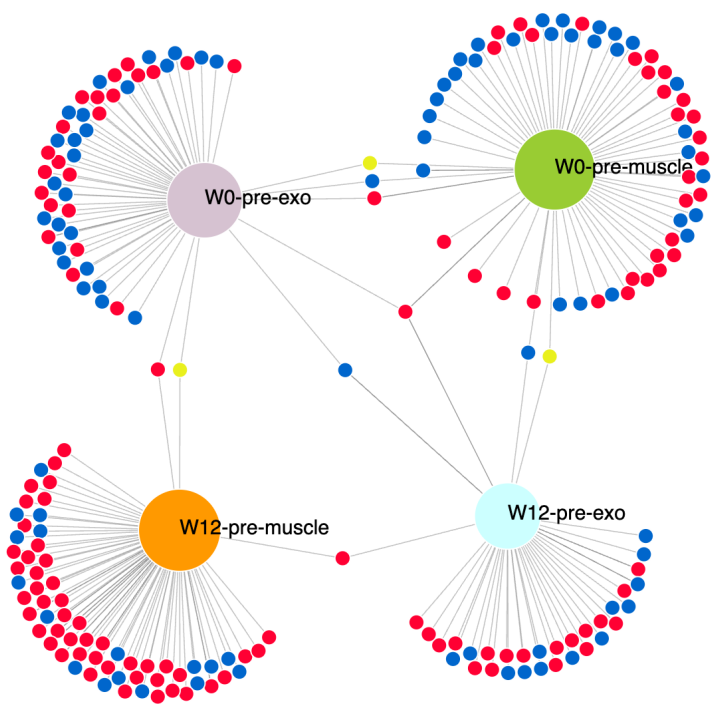

E.

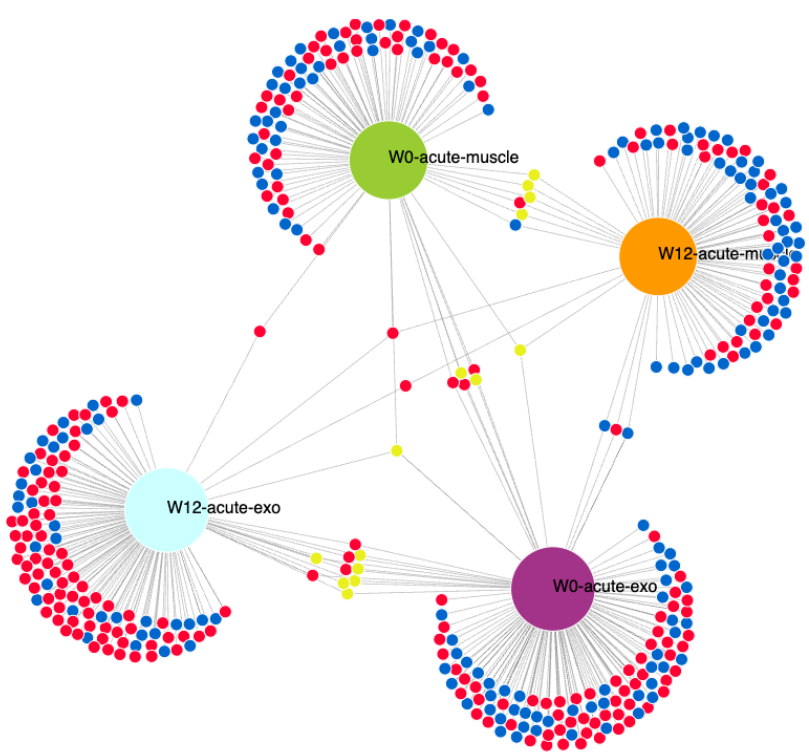

F.

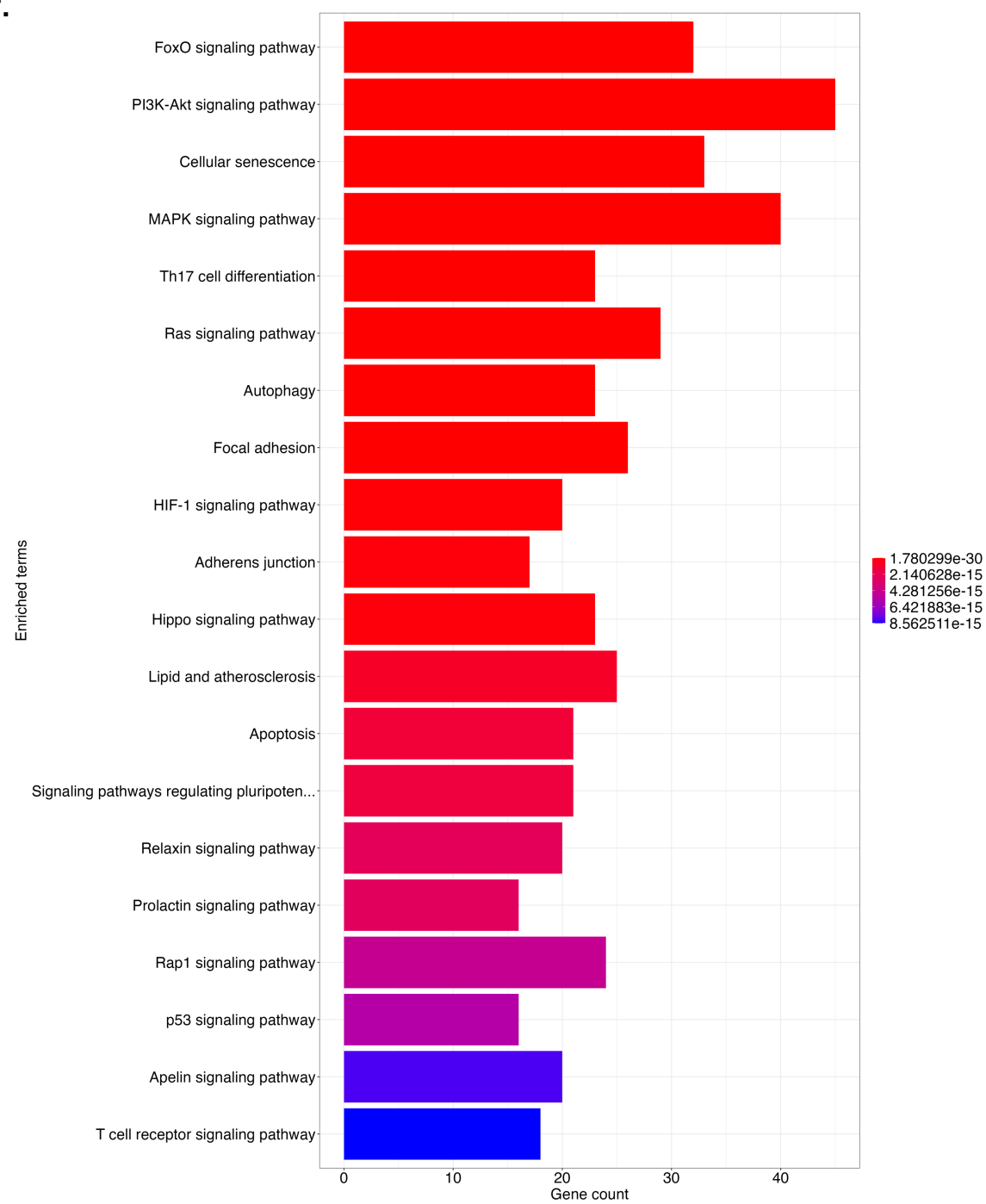

A.

miRNA	Tissue in DGE	Tissue in HOSVD	Differential Response
miR-656-3p	Exosome	Muscle	Acute response in untrained state
miR-3622b-5p	Muscle	Muscle	
miR-589-5p	Exosome	Exosome	Acute response in trained state
miR-95-3p	Exosome	Exosome	
miR-935	Exosome	Muscle	Training response
miR-1296-5p	Muscle	Muscle	
miR-376a-5p	Muscle	Exosome	
miR-338-5p	Exosome	Muscle	
miR-181d-5p	Exosome, Muscle	Exosome	

B.

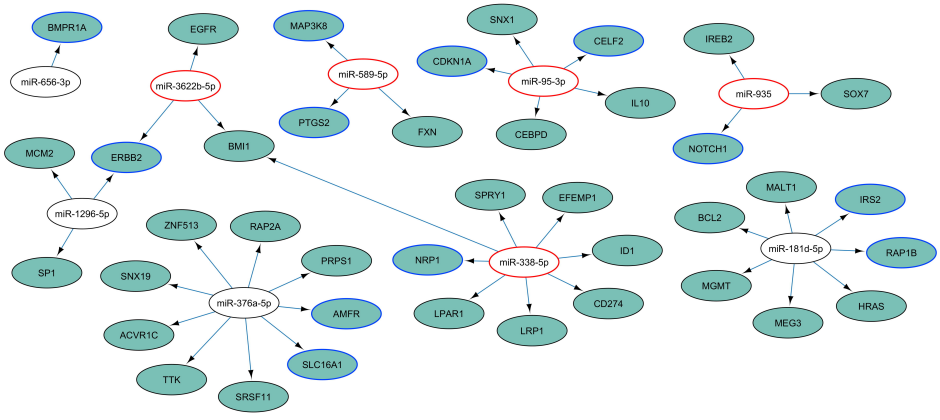
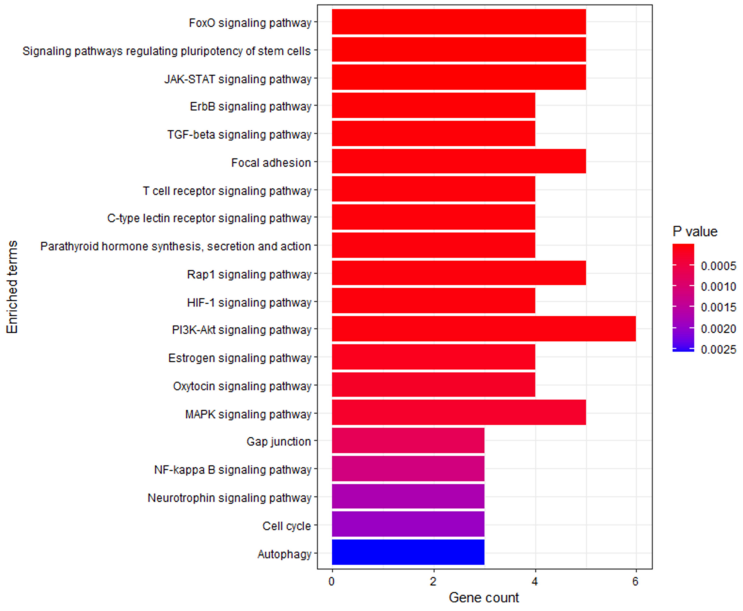
C.